

Measurement of the $t\bar{t}$ production cross-section in the lepton+jets channel at $\sqrt{s}=13$ TeV with the ATLAS experiment

ATLAS Collaboration; Newman, Paul

DOI:

[10.1016/j.physletb.2020.135797](https://doi.org/10.1016/j.physletb.2020.135797)

License:

Creative Commons: Attribution (CC BY)

Document Version

Publisher's PDF, also known as Version of record

Citation for published version (Harvard):

ATLAS Collaboration & Newman, P 2020, 'Measurement of the $t\bar{t}$ production cross-section in the lepton+jets channel at $\sqrt{s}=13$ TeV with the ATLAS experiment', *Phys. Lett. B*, vol. 810, 135797.

<https://doi.org/10.1016/j.physletb.2020.135797>

[Link to publication on Research at Birmingham portal](#)

General rights

Unless a licence is specified above, all rights (including copyright and moral rights) in this document are retained by the authors and/or the copyright holders. The express permission of the copyright holder must be obtained for any use of this material other than for purposes permitted by law.

- Users may freely distribute the URL that is used to identify this publication.
- Users may download and/or print one copy of the publication from the University of Birmingham research portal for the purpose of private study or non-commercial research.
- User may use extracts from the document in line with the concept of 'fair dealing' under the Copyright, Designs and Patents Act 1988 (?)
- Users may not further distribute the material nor use it for the purposes of commercial gain.

Where a licence is displayed above, please note the terms and conditions of the licence govern your use of this document.

When citing, please reference the published version.

Take down policy

While the University of Birmingham exercises care and attention in making items available there are rare occasions when an item has been uploaded in error or has been deemed to be commercially or otherwise sensitive.

If you believe that this is the case for this document, please contact UBIRA@lists.bham.ac.uk providing details and we will remove access to the work immediately and investigate.



Measurement of the $t\bar{t}$ production cross-section in the lepton+jets channel at $\sqrt{s} = 13$ TeV with the ATLAS experiment

The ATLAS Collaboration^{*}

ARTICLE INFO

Article history:

Received 24 June 2020

Received in revised form 4 September 2020

Accepted 17 September 2020

Available online 22 September 2020

Editor: M. Doser

ABSTRACT

The top anti-top quark production cross-section is measured in the lepton+jets channel using proton–proton collision data at a centre-of-mass energy of $\sqrt{s} = 13$ TeV collected with the ATLAS detector at the LHC. The dataset corresponds to an integrated luminosity of 139 fb^{-1} . Events with exactly one charged lepton and four or more jets in the final state, with at least one jet containing b -hadrons, are used to determine the $t\bar{t}$ production cross-section through a profile-likelihood fit. The inclusive cross-section is measured to be $\sigma_{\text{inc}} = 830 \pm 0.4 \text{ (stat.)} \pm 36 \text{ (syst.)} \pm 14 \text{ (lumi.) pb}$ with a relative uncertainty of 4.6%. The result is consistent with theoretical calculations at next-to-next-to-leading order in perturbative QCD. The fiducial $t\bar{t}$ cross-section within the experimental acceptance is also measured.

© 2020 The Author(s). Published by Elsevier B.V. This is an open access article under the CC BY license (<http://creativecommons.org/licenses/by/4.0/>). Funded by SCOAP³.

1. Introduction

The top quark is the heaviest elementary particle in the Standard Model (SM), with a mass m_t close to the electroweak symmetry breaking scale [1,2]. Studies of top-quark production and decays provide a precise probe of the SM as well as its extensions [3]. At the CERN Large Hadron Collider (LHC), top quarks are primarily produced in quark–antiquark pairs ($t\bar{t}$) and form an important background in many searches for physics beyond the SM. Thus, a precise measurement of the $t\bar{t}$ cross-section, and comparison with theoretical predictions of high precision, are a critical part of the LHC physics programme.

A theoretical calculation of the $t\bar{t}$ cross-section, $\sigma_{t\bar{t}}$, is available at next-to-next-to-leading order (NNLO) in quantum chromodynamics (QCD). It includes the resummation of the next-to-next-to-leading logarithmic (NNLL) soft-gluon terms [4–9] and predicts $\sigma_{t\bar{t}} = 832_{-29}^{+20} \text{ (scale)} \pm 35 \text{ (PDF} + \alpha_s) \text{ pb}$ in proton–proton (pp) collisions at a centre-of-mass energy of 13 TeV, as calculated by the Top++ (v2.0) program [10], using the MSTW2008 NNLO PDF set [11,12] as the central PDF set and assuming $m_t = 172.5 \text{ GeV}$. The scale uncertainty was determined from the envelope of predictions with the QCD renormalisation and factorisation scales varied independently up or down by a factor of two. The combined uncertainty due to the parton distribution functions (PDFs) and the strong coupling constant, α_s , was calculated following the PDF4LHC prescription [13] with the MSTW2008 NNLO, CT10 NNLO [14,15] and NNPDF2.3 5fFFN NNLO [16] PDF sets.

Measurements of inclusive $\sigma_{t\bar{t}}$ at 7, 8 and 13 TeV were performed by both the ATLAS [17–19] and CMS [20–24] collaborations. All measurements are consistent with NNLO+NNLL QCD predictions. Additionally, the CMS Collaboration performed a measurement of $\sigma_{t\bar{t}}$ at $\sqrt{s} = 5.02 \text{ TeV}$ [25]. At $\sqrt{s} = 13 \text{ TeV}$, the ATLAS Collaboration used a data sample of 36.1 fb^{-1} and events with an opposite-charge electron–muon pair in the final state to obtain $\sigma_{t\bar{t}} = 826.4 \pm 3.6 \text{ (stat.)} \pm 11.5 \text{ (syst.)} \pm 15.7 \text{ (lumi.)} \pm 1.9 \text{ (beam) pb}$ [26], giving a total relative uncertainty of 2.4%.

This Letter documents measurements of the $t\bar{t}$ cross-sections in the full phase space (inclusive) and in a phase space defined to be close to the experimental measurement range (fiducial) at $\sqrt{s} = 13 \text{ TeV}$, using the full pp dataset collected during 2015–2018. It targets the lepton+jets $t\bar{t}$ decay mode, where one W boson originating from the top quark decays leptonically and the other W boson decays hadronically, i.e. $t\bar{t} \rightarrow W^+W^-b\bar{b} \rightarrow \ell\nu q\bar{q}'b\bar{b}$, producing a final state with one high-momentum electron or muon and four jets, two of which are b -quark-initiated jets.¹ A small contribution from $t\bar{t}$ events with both W bosons decaying leptonically producing the same final state due to one lepton being out of acceptance is treated as signal. A profile-likelihood fit to data in three non-overlapping regions is employed to perform the measurement.

The study presented in this letter probes a final state that is complementary to the one explored in Ref. [26] and is sensitive to different $t\bar{t}$ modelling uncertainties, e.g. uncertainties related to quark jets, the understanding of which is mandatory for a large

^{*} E-mail address: atlas.publications@cern.ch.

¹ Events involving $W \rightarrow \tau\nu$ decays with a subsequent decay of the τ -lepton into $e\nu_e\nu_\tau$ or $\mu\nu_\mu\nu_\tau$ are included in the signal.

number of top-quark precision measurements and searches beyond the SM.

2. ATLAS detector

ATLAS [27–29] is a multipurpose particle detector designed with a forward–backward symmetric cylindrical geometry and nearly full 4π coverage in solid angle.² It consists of an inner tracking detector surrounded by a thin superconducting solenoid providing a 2 T axial magnetic field, electromagnetic and hadronic calorimeters, and a muon spectrometer. The inner tracking detector covers the pseudorapidity range $|\eta| < 2.5$ and is composed of silicon pixel, silicon microstrip, and transition radiation tracking (TRT) detectors. Lead/liquid-argon (LAr) sampling calorimeters provide electromagnetic (EM) energy measurements with high granularity. Hadronic calorimetry is provided by the steel/scintillator-tile calorimeter covering the central pseudorapidity range ($|\eta| < 1.7$). The endcap and forward regions are instrumented with LAr calorimeters for both the EM and hadronic energy measurements up to $|\eta| = 4.9$. The muon spectrometer surrounds the calorimeters and is based on three large air-core toroidal superconducting magnets with eight coils each. The field integral of the toroids ranges between 2.0 and 6.0 Tm across most of the detector. The muon spectrometer includes a system of precision tracking chambers and fast detectors for triggering. A two-level trigger system is used to select events. The first-level trigger is implemented in hardware and uses a subset of the detector information to keep the accepted event rate below 100 kHz [30]. This is followed by a software-based trigger that reduces the accepted event rate to 1 kHz on average.

3. Data and simulation samples

The analysis is performed using the full Run 2 LHC pp collision data sample at $\sqrt{s} = 13$ TeV recorded by the ATLAS detector, corresponding to an integrated luminosity of 139 fb^{-1} after data quality requirements [31] are imposed. Events are required to pass a single-electron or single-muon trigger with thresholds that were progressively raised during the data collection period to account for the increase of instantaneous luminosity.

Monte Carlo (MC) simulations are used to optimise the analysis and to evaluate acceptances, efficiencies and uncertainties in $t\bar{t}$ signal and all backgrounds except for the multijet background that is estimated using a data-driven technique. The effect of multiple interactions in the same and neighbouring bunch crossings (pile-up) was modelled by overlaying the original hard-scattering event with simulated inelastic pp events generated by PYTHIA 8.186 [32] using the NNPDF2.3 LO set of PDFs [16] and parameter values set according to the A3 tune [33].

The production of $t\bar{t}$ events was modelled using the next-to-leading-order (NLO) matrix element (ME) implemented in the HVQ program [34,35] from the POWHEG-Box v2 [36–38] generator with the NNPDF3.0 NLO [39] PDF and the h_{damp} parameter set to $1.5 m_t$ [40].³ The $t\bar{t}$ sample is normalised to the NNLO+NNLL cross-section. The single-top-quark t -channel, s -channel and tW associated production processes were also modelled at NLO in QCD using

POWHEG-Box v2. For all top-quark processes, PYTHIA 8.230 [41], using the A14 tune [42] and the NNPDF2.3 LO PDF set, was interfaced to POWHEG-Box v2 to simulate the parton shower and hadronisation. The diagram removal scheme [43] was employed in the tW simulation to handle the interference with $t\bar{t}$ production [40].

The V +jets ($V = W, Z$) backgrounds were simulated with the SHERPA v2.2.1 [44] generator using NLO-accurate MEs for up to two jets, and MEs accurate to leading order (LO) for up to four jets calculated with the Comix [45] and OpenLoops [46,47] libraries. They were matched with the SHERPA parton shower [48] using the MEPS@NLO prescription [49–52] and the tune developed by the SHERPA authors. Diboson production was generated using SHERPA v2.2.2 with MEs computed at NLO accuracy in QCD for up to one additional parton and at LO accuracy for up to three additional partons. The NNPDF3.0 NNLO PDF set [39] was used for the V +jets and diboson samples. The productions of $t\bar{t}H$ and $t\bar{t}V$ events were modelled at NLO using the POWHEG-Box v2 and MADGRAPH5_aMC@NLO v2.3.3 [53] generators, respectively, with the NNPDF3.0 NLO PDF set. PYTHIA 8.230 with the A14 tune and the NNPDF2.3 LO PDF was used to simulate the parton showers.

All simulated background samples are normalised to their cross-sections, computed to the highest order available in perturbation theory. The top-quark mass is set to $m_t = 172.5$ GeV in all simulated samples. The EvtGEN v1.6.0 program [54] was used to simulate the decay of bottom and charm hadrons for all event generators except SHERPA.

The nominal $t\bar{t}$ signal and background samples were processed through the ATLAS simulation software [55] based on GEANT4 [56]. Some of the alternative $t\bar{t}$ samples used to evaluate systematic uncertainties were processed through a fast detector simulation making use of parameterised showers in the calorimeters [57]. Corrections are applied to the simulated events so that the selection efficiencies, energy scales and resolutions of particle candidates match those determined from data control samples.

4. Object selection

The following sections describe the detector- and particle-level objects used in the inclusive and fiducial cross-section measurements.

4.1. Detector-level objects

Electron candidates are reconstructed from energy clusters in the EM calorimeter that match a reconstructed track. Electrons are identified with a likelihood method [58], and are required to meet the tight identification criterion based on shower shapes in the EM calorimeter, track quality and detection of transition radiation produced in the TRT. Electrons are required to have a calorimeter cluster satisfying $|\eta_{\text{clust}}| < 2.47$. Additionally, electrons in the transition region between barrel and endcap calorimeters with $1.37 < |\eta_{\text{clust}}| < 1.52$ are excluded. The electron candidates have to pass p_T - and η -dependent isolation requirements based on the track and calorimeter activity around them. Muons are reconstructed using information from both the inner detector and the muon spectrometer. Muon candidates are required to have $|\eta| < 2.5$, to pass medium quality requirements [59] and fulfil isolation criteria based on the calorimeter and tracking information: the calorimeter cluster energy within a cone of size of $\Delta R = 0.2$ around the muon track divided by the muon p_T must be smaller than 0.15 and the ratio of the summed transverse momenta of additional tracks within a cone of $\Delta R = 0.3$ to the muon p_T must be smaller than 0.04. Selected electrons (muons) must have a transverse impact parameter significance $|d_0/\sigma_{d_0}| < 5$ (3) and a longitudinal impact parameter $|z_0 \sin \theta| < 0.5$ mm relative to the event's primary vertex [60].

² ATLAS uses a right-handed coordinate system with its origin at the nominal interaction point (IP) in the centre of the detector and the z -axis along the beam pipe. The x -axis points from the IP to the centre of the LHC ring, and the y -axis points upwards. Cylindrical coordinates (r, ϕ) are used in the transverse plane, ϕ being the azimuthal angle around the z -axis. The pseudorapidity is defined in terms of the polar angle θ as $\eta = -\ln \tan(\theta/2)$. Angular distance is measured in units of $\Delta R \equiv \sqrt{(\Delta\eta)^2 + (\Delta\phi)^2}$.

³ The h_{damp} parameter controls the transverse momentum, p_T , of the first additional emission beyond the leading-order Feynman diagram in the parton shower and therefore regulates the high- p_T emission against which the $t\bar{t}$ system recoils.

Table 1

Expected event yields including all uncertainties after the event selection compared to data in the three signal regions. The $t\bar{t}X$ category contains $t\bar{t}V$ and $t\bar{t}H$ contributions.

	SR1	SR2	SR3
$t\bar{t}$	$3\,630\,000 \pm 210\,000$	$990\,000 \pm 90\,000$	$980\,000 \pm 100\,000$
W +jets	$350\,000 \pm 160\,000$	$24\,000 \pm 10\,000$	$17\,000 \pm 9000$
Single top	$255\,000 \pm 31\,000$	$52\,000 \pm 7000$	$37\,000 \pm 8000$
Z +jets & diboson	$80\,000 \pm 40\,000$	8000 ± 4000	5800 ± 3000
$t\bar{t}X$	$15\,600 \pm 2100$	2110 ± 290	7200 ± 1000
Multijet	$210\,000 \pm 80\,000$	$28\,000 \pm 10\,000$	$22\,000 \pm 8000$
Total prediction	$4\,540\,000 \pm 310\,000$	$1\,110\,000 \pm 100\,000$	$1\,070\,000 \pm 100\,000$
Data	4 540 886	1 100 558	1 103 317

Jets are formed from clusters of topologically connected calorimeter cells [61] using the anti- k_t jet algorithm [62] with the radius parameter $R = 0.4$ implemented in FastJet [63], and are calibrated to particle level as described in Ref. [64]. To suppress jets originating from pile-up collisions, cuts on the Jet Vertex Tagger (JVT) [65] discriminant are applied for jets with p_T below 120 GeV. Jets containing b -hadrons are identified (b -tagged) via a multivariate algorithm, MV2c10, combining observables sensitive to lifetimes, production mechanisms, and decay properties of b -hadrons [66]. A working point with an average efficiency of 60% for b -quark-initiated jets in $t\bar{t}$ events and rejection factors against light-quark/gluon-initiated jets and c -quark-initiated jets of 1200 and 55, respectively, is used [67–69].

The missing transverse momentum with magnitude, E_T^{miss} , is defined as the negative vector sum of the transverse momenta of the reconstructed and calibrated physics objects (electrons, photons, hadronically decaying τ -leptons, jets and muons) and a soft term built from all tracks that are associated with the primary vertex, but not with these objects, is included [70,71].

4.2. Particle-level objects

Particle-level objects are defined in simulated events by using only stable particles, i.e. particles with a mean lifetime greater than 30 ps. The fiducial phase space used for the $\sigma_{t\bar{t}}$ measurement is defined using a set of requirements applied to particle-level objects analogous to those used in the selection of the detector-level objects.

Leptons are defined as electrons or muons originating from W decays, including those from intermediate τ -leptons. The four-momentum of each charged lepton is summed with the four-momenta of all radiated photons within a cone of size $\Delta R = 0.1$ about its direction, excluding photons from hadron decays, to account for bremsstrahlung. Leptons are required to have $p_T > 25$ GeV and $|\eta| < 2.5$. Jets are defined using the anti- k_t algorithm with a radius parameter of $R = 0.4$. All stable particles are considered for jet clustering, except for the electrons, muons, and photons used in the lepton definitions. Jets are required to have $p_T > 25$ GeV and $|\eta| < 2.5$ and are identified as b -jets via ghost matching to weakly decaying b -hadrons [62]. The fiducial region is defined by requiring exactly one electron or muon, and at least four jets, one or exactly two of which must be identified as b -jets.

Possible double-counting of objects reconstructed at detector- or particle-levels satisfying multiple object definitions is resolved using the same algorithms as in Ref. [72].

5. Analysis strategy

5.1. Event selection

Selected events are required to have exactly one reconstructed electron or muon with $p_T > 25$ GeV for the 2015 data-taking

period, $p_T > 27$ GeV for the 2016 data-taking period and $p_T > 28$ GeV for the 2017 and 2018 data-taking periods, to account for different single-lepton trigger thresholds. Events must have at least four reconstructed jets with $p_T > 25$ GeV and $|\eta| < 2.5$ with one or exactly two of the reconstructed jets being b -tagged. To suppress the contribution of the multijet background, events in the electron+jets channel are required to have $E_T^{\text{miss}} > 30$ GeV and $m_T(W) > 30$ GeV, while in the muon+jets channel, due to a smaller contribution of this background, a looser criterion $E_T^{\text{miss}} + m_T(W) > 60$ GeV is applied.⁴ The measurement of the $t\bar{t}$ cross-section is performed by splitting the selected sample into three non-overlapping signal regions according to the number of jets and b -tagged jets. The region with the highest background fraction (SR1) is selected by requiring ≥ 4 jets and exactly 1 b -tagged jet. The SR2 (SR3) region has exactly 4 (≥ 5) jets, exactly two of which must be b -tagged. The SR1 and SR2 regions have different sensitivities to the background and b -jet modelling while the SR3 provides information about modelling of extra radiation in $t\bar{t}$ events.

The number of background events meeting the selection criteria is estimated using MC simulations for all processes with the exception of a small contribution from multijet events with a non-prompt or misidentified lepton arising from photon conversions, heavy-flavour hadrons decaying leptonically, and jets misidentified as leptons. A data-driven matrix method [72] based on the measurement of lepton selection efficiencies using different identification and isolation criteria is used to estimate this background. Expected and observed event yields are shown in Table 1 and are in excellent agreement. The expected yields include all uncertainties described in Section 6.

5.2. Observables used in the fit

The $t\bar{t}$ cross-section is extracted from a simultaneous profile-likelihood fit of data distributions to the sum of signal and background distributions in the three regions. Each region exploits a different fit variable. In SR1, the aplanarity (A) is used, as was done in previous $t\bar{t}$ cross-section measurements [73,74]. It is defined entirely with jet information as $A = \frac{3}{2}\lambda_3$, where λ_3 is the smallest eigenvalue of the sphericity tensor, $S^{\alpha\beta}$ [75,76].⁵ In SR2, the minimum lepton-jet mass, $m_{\ell j}^{\text{min}}$, calculated as the minimum invariant mass over all lepton-jet pairs, is exploited. In SR3, a system likely originating from a hadronically decaying top quark is constructed. It consists of a b -tagged jet and two other jets, corresponding to the permutation with the highest p_T for the vector

⁴ $m_T(W) = \sqrt{2p_T^\ell E_T^{\text{miss}}(1 - \cos\phi)}$, where p_T^ℓ is the transverse momentum of the charged lepton and ϕ is the opening azimuthal angle between the charged lepton and missing transverse momenta.

⁵ The $S^{\alpha\beta} = \frac{\sum_i p_i^\alpha p_i^\beta}{\sum_i |p_i|^2}$, where p_i represents the three-momentum of jet i ; $\alpha, \beta \in x, y, z$ and the sum runs over all jets.

sum of four momenta of the three constituent jets. The average angular distance between the three constituent jets, $\Delta R_{bjj}^{\text{avg}}$, is computed and used in the fit. The choice of variables is driven by their ability to separate $t\bar{t}$ signal from the backgrounds, the reduced sensitivity to jet-related experimental and $t\bar{t}$ modelling uncertainties achieved by exploiting ratios of jet momenta (A) or angular information ($\Delta R_{bjj}^{\text{avg}}$), and good agreement between the prediction and data. There is no single variable that satisfies these requirements in all three regions.

6. Systematic uncertainties

Several sources of systematic uncertainties affect the fiducial and inclusive $t\bar{t}$ cross-section measurements by changing the estimated signal and background rates and the shapes of the distributions used in the fit. All uncertainties are treated as correlated between signal regions, unless explicitly specified otherwise. They can be classified into experimental and modelling uncertainties in the $t\bar{t}$ signal and in backgrounds.

6.1. Experimental uncertainties

The uncertainty in the combined 2015–2018 integrated luminosity (\mathcal{L}_{int}) is 1.7% [77], obtained using the LUCID-2 detector [78] for the primary luminosity measurements.

Reconstruction, identification, isolation and trigger performance for electrons and muons differ between data and MC simulations. Scale factors are applied to simulated events to correct for the differences. These scale factors, as well as the lepton momentum scale and resolution, are assessed using $Z \rightarrow \ell^+ \ell^-$ events in simulation and data with methods similar to those described in Refs. [58,59]. The associated systematic uncertainties are propagated to the distributions used in the fit. Their combined effects on the cross-section measurement are referred to as “Muon reconstruction” and “Electron reconstruction” in Table 3.

The jet energy scale (JES) is calibrated using a combination of test beam data, simulation and *in situ* techniques [64]. Its uncertainty is decomposed into a set of 29 uncorrelated components, with contributions from pile-up, jet flavour composition, single-particle response, and effects of jets not contained within the calorimeter. The uncertainty of the jet energy resolution (JER) is represented by eight components accounting for jet- p_T and η -dependent differences between simulation and data [79]. The uncertainty in the efficiency to pass the JVT requirement for pile-up suppression is also considered [65]. The combined effect on the cross-section measurement of jet-related uncertainties is referred to as “Jet reconstruction” in Table 3.

The uncertainties in the b -tagging calibration are determined separately for b -jets, c -jets and light-flavour-jets [66,68,69] using an 85-component breakdown (45 for b -jets, 20 for c -jets and 20 for light-flavour jets). They depend on p_T for b - and c -jets, and on p_T and η for light-flavour jets, and they account for differences between data and simulation. The impact of these uncertainties on the cross-section measurement is referred to as “Flavour tagging” in Table 3.

The uncertainty in E_T^{miss} due to a possible miscalibration of its soft-track component is derived from data–simulation comparisons of the p_T balance between the hard and the soft E_T^{miss} components [70]. To account for the difference in pile-up distributions between the simulation and data, the pile-up profile in the simulation is corrected to match the one in data. The uncertainty associated with the correction factor is applied. The combined impact of the E_T^{miss} and pile-up uncertainties is referred to as “ E_T^{miss} + pile-up” in Table 3.

6.2. Signal modelling

The uncertainty due to missing higher-order QCD corrections in the ME computation is estimated by independently varying the renormalisation (μ_R) and factorisation (μ_F) scales by factors of 2.0 and 0.5 with respect to the central value. Additionally, uncertainties in the amounts of initial- and final-state radiation (FSR) from the parton shower are assessed by, respectively varying the corresponding parameter of the A14 parton shower tune (Var3c) [42] and by varying by factors of 2.0 and 0.5 the scale μ_R^{FSR} . All four variations are taken to be uncorrelated between the signal regions but fully correlated across bins in each region. The combined impact of all scale uncertainties is referred to as “ $t\bar{t}$ scale variations” in Table 3. An uncertainty due to the choice of the h_{damp} parameter value is determined by comparing the nominal $t\bar{t}$ sample with the one produced with the same settings but with the h_{damp} parameter set to $3 m_t$ and is symmetrised.

The level of agreement between data and prediction for the lepton p_T and the leading jet p_T improves if the top-quark p_T distribution in the nominal $t\bar{t}$ simulation is corrected to match the top-quark p_T calculated at NNLO in QCD with NLO electroweak corrections [80]. In this analysis, the full difference between the nominal and the reweighted simulated $t\bar{t}$ sample is taken as a systematic uncertainty and symmetrised. This approach is preferable to applying a correction to the nominal simulation because for some variables the level of agreement between data and prediction deteriorates after applying the correction. To avoid double counting, modelling uncertainties, which are evaluated using alternative samples, are derived as the difference between the nominal and alternative samples, both reweighted to the top-quark p_T theory prediction.

Uncertainties due to the choice of parton shower and hadronisation model are estimated by comparing the nominal sample from POWHEG-Box interfaced to PYTHIA with an alternative sample generated with the same POWHEG-Box set-up but interfaced to HERWIG 7.0.4 [81,82] with angle-ordered parton shower model, the H7UE tune [81] and the MMHT2014LO PDF set [83]. Further details about the sample settings can be found in Ref. [84]. The difference between the two models is split into three components. The first component represents the total $t\bar{t}$ acceptance in the three regions (“Shower model incl. acceptance” in Fig. 3). The second component is sensitive to the $t\bar{t}$ yield difference in the individual signal regions (“Shower migration parameter” in Fig. 3). The last component is responsible for the shape effect on the fitted distributions. It is represented by three nuisance parameters (NPs), one per region (referred to as “Shower model shape” followed by a region name in Fig. 3), to ensure that shape effects are uncorrelated between the regions since different variables are used in the fit. All three components are symmetrised. The combined impact of all uncertainties due to the choice of parton shower and hadronisation model is referred to as “ $t\bar{t}$ shower/hadronisation” in Table 3.

The PDF4LHC15 meta-PDFs are used to estimate the systematic effects, including impact on the acceptance, due to uncertainties in the PDF, following the updated PDF4LHC15 prescription [85]. A set of 30 Hessian eigenvectors corresponding to independent PDF variations is included in the fit. The central values of the NNPDF3.0 PDF used to simulate the nominal $t\bar{t}$ sample and the PDF4LHC15 set are found to be consistent.

6.3. Background modelling

Uncertainties in the multijet background estimation include a 50% uncertainty in the normalisation to cover differences between the data and the matrix method prediction in various control regions enriched in multijet background events [72] and an uncertainty from the choice of parameterisation of the efficiencies for

real and misidentified leptons. These uncertainties are treated as uncorrelated between all regions and between electron+jets and muon+jets events due to different composition of the multijet background in these regions and different choice of efficiency parameterisation in the electron+jets and muon+jets channels. The impact of the multijet background estimation uncertainty on the measurement is referred to as “Multijet background” in Table 3.

The tW contribution is the largest among the three single-top-quark production channels. A normalisation uncertainty of 5.4% is applied to the single-top-quark background, corresponding to the theoretical uncertainty of the tW cross-section [86]. Similarly to the $t\bar{t}$ modelling uncertainties, the effects of the μ_R and μ_F variations in the ME, the variations of parameters related to initial- and final-state radiation in the parton shower and the impact of the parton shower choice are evaluated for the single-top-quark background. An additional uncertainty arising from the method used to handle interference between tW and $t\bar{t}$ production is determined by comparing the tW simulated sample that uses the diagram-subtraction method [87] with the nominal one based on the diagram-removal technique.

Several uncertainties affect the modelling of the W +jets background. Variations of μ_R and μ_F are used to derive the W +jets normalisation uncertainties in each region. They amount to about 45% and are treated as uncorrelated between the regions selected with 1- b -tag (SR1) and 2- b -tag (SR2 and SR3) requirements. The effects on the shape of the distributions arising from the μ_R and μ_F variations, from the choice of ME to parton-shower CKKW matching scale [51,88] and from the scale used for the resummation of soft-gluon emission in the nominal sample are also included.

A normalisation uncertainty of 50% is applied to the combined Z +jets and diboson background based on the studies of the μ_R and μ_F variations for the W +jets process. A normalisation uncertainty of 13.3% is applied [89] to the $t\bar{t}X$ contribution, based on the theoretical cross-section uncertainties for the $t\bar{t}V$ and $t\bar{t}H$ processes.

For the backgrounds, the systematic uncertainties due to the PDF choice are found to be negligible. The combined effect on the measured cross-section of all MC simulation background modelling uncertainties is referred to as “MC background modelling” in Table 3.

7. Extraction of the $t\bar{t}$ cross-section

Events fulfilling the criteria described in Section 5 are used to perform measurements of the fiducial and inclusive $t\bar{t}$ cross-sections from a profile-likelihood fit to data. The fit uses the distributions of variables described in Section 5.2 in three signal regions, and the systematic uncertainties (see Section 6) are included in the fit as NPs. Statistical uncertainties in each bin due to the limited size of the simulated samples are taken into account by dedicated nuisance parameters using the Barlow-Beeston technique [90] and their effect on the measurement is referred to as “Simulation stat. uncertainty” in Table 3.

The cross-section for producing $t\bar{t}$ events in the fiducial region, σ_{fid} , is defined as $\sigma_{\text{fid}} = \nu_{\text{fid}}/L_{\text{int}}$, where ν_{fid} is the number of $t\bar{t}$ events in the fiducial volume determined by the fit. The inclusive cross-section, σ_{inc} , is related to the fiducial one via $\sigma_{\text{fid}} = A_{\text{fid}} \times \sigma_{\text{inc}}$, where $A_{\text{fid}} = N_{\text{fid}}/N_{\text{tot}}$ is the fiducial acceptance with N_{fid} (N_{tot}) being the number of $t\bar{t}$ events obtained from a simulated signal sample after (before) applying the particle-level selection. For the σ_{fid} measurement, all samples of simulated events used to evaluate the $t\bar{t}$ modelling uncertainties are scaled to the same fiducial acceptance, defined in Section 4.2. The fiducial acceptance is evaluated using the nominal $t\bar{t}$ sample reweighted to match the top-quark p_T theoretical calculation to be consistent with the treatment of the alternative $t\bar{t}$ samples. Such scaling

Table 2

Fiducial acceptances for different $t\bar{t}$ models, with the variations relative to the nominal model, after applying the particle-level event selection. The uncertainty in the acceptance due to each systematic variation ($A_{\text{fid}}^{\text{alt}}$) is computed with respect to the acceptance obtained from the nominal $t\bar{t}$ sample reweighted to the NNLO theory prediction of the top-quark p_T given in the second row ($A_{\text{fid}}^{\text{nom}}$). The PDF uncertainty is a sum in quadrature of uncertainties from 30 independent PDF variations in the PDF4LHC15 prescription. The last row shows the total relative uncertainty in the nominal acceptance.

Generator set-up	A_{fid} [%]	$\frac{A_{\text{fid}}^{\text{alt}} - A_{\text{fid}}^{\text{nom}}}{A_{\text{fid}}^{\text{nom}}}$ [%]
POWHEG+PYTHIA nominal	13.50	0.00
POWHEG+PYTHIA top-quark p_T reweighted	13.40	−0.75
$\mu_R^{\text{FSR}} \times 2$	13.58	1.29
$\mu_R^{\text{FSR}} \times 0.5$	13.18	−1.64
$\mu_R \times 2$	13.37	−0.25
$\mu_R \times 0.5$	13.45	0.38
$\mu_F \times 2$	13.38	−0.15
$\mu_F \times 0.5$	13.43	0.17
Var3cUp	13.46	0.41
Var3cDown	13.35	−0.38
$h_{\text{damp}} \times 2$	13.57	1.21
POWHEG+HERWIG	13.44	0.31
PDF4LHC15 variations		0.47
Total		+1.9 −2.2

ensures that in each signal region the remaining normalisation uncertainties from $t\bar{t}$ modelling correspond to the uncertainties in the correction factor $C = N_{\text{reco}}/N_{\text{fid}}$, where N_{reco} is the number of selected events in a given region. The scaled distributions enter the fit to measure σ_{fid} , thus reducing the impact of $t\bar{t}$ modelling uncertainties by reducing the normalisation effects. For the σ_{inc} extraction, the $t\bar{t}$ modelling uncertainties include the uncertainties corresponding to the extrapolation of each systematic uncertainty component to the full phase space. The acceptance A_{fid} for different systematic variations of the $t\bar{t}$ model is shown in Table 2. The PDF uncertainty is calculated following the PDF4LHC15 prescription as a sum in quadrature of uncertainties from 30 independent PDF variations. The relative acceptance uncertainty in the propagation of the fiducial cross-section to the full phase space for the nominal $t\bar{t}$ model is $+1.9\%$ -2.2% .

8. Results

The $t\bar{t}$ fiducial cross-section is found to be

$$\sigma_{\text{fid}} = 110.7 \pm 0.05 \text{ (stat.) } {}^{+4.5}_{-4.3} \text{ (syst.)} \pm 1.9 \text{ (lumi.) pb} \\ = 110.7 \pm 4.8 \text{ pb.}$$

Here, the luminosity uncertainty is obtained by repeating the fit, fixing the corresponding nuisance parameter, and subtracting in quadrature the resulting uncertainty from the total uncertainty of the nominal fit. The systematic uncertainty is determined by subtracting in quadrature the statistical uncertainty, obtained from a fit where all NPs are fixed to the values determined by the fit (post-fit), and the luminosity uncertainty, from the total uncertainty. Fig. 1 displays the post-fit distributions of the observables used in the fit in each region.

Fig. 2 shows pre- and post-fit distributions of one kinematic variable per region, which is not included in the fit, demonstrating that the level of agreement between the prediction and the data improves after the fit. The H_T distribution shows a difference between prediction and data, which is covered by the uncertainties both before and after the fit. This feature has no effect on the variables used in the fit or on the result. The effect of the residual disagreement in the distribution of the fourth largest jet p_T in SR2, which is not fully covered by the post-fit uncertainty

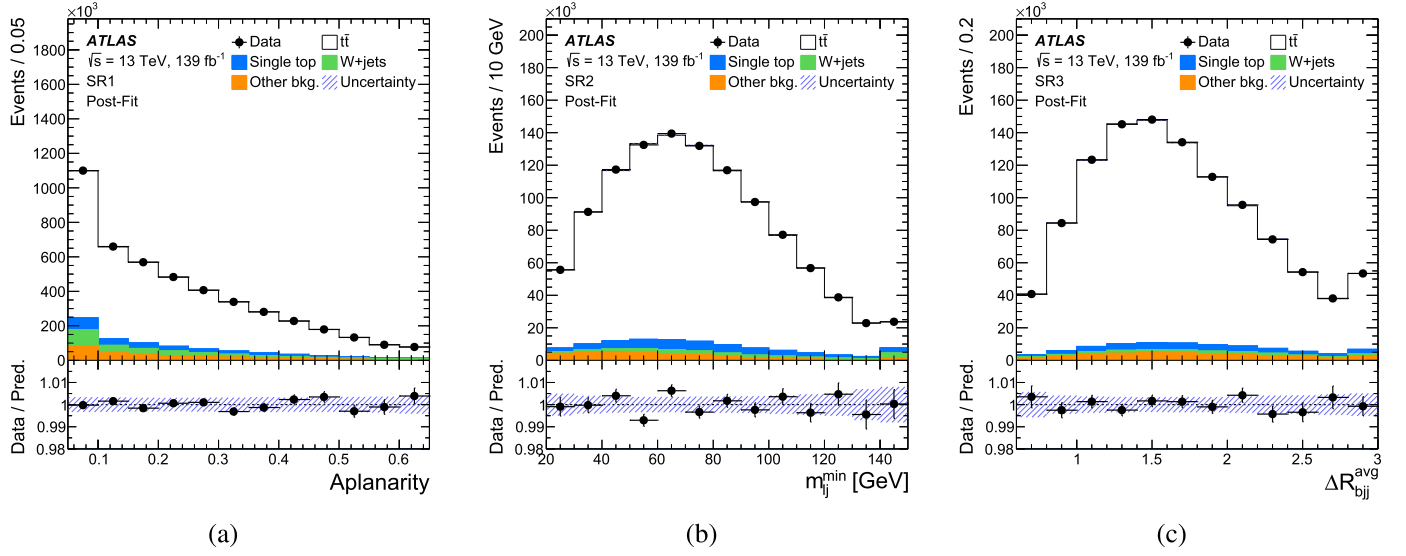


Fig. 1. Post-fit distributions of $t\bar{t}$ signal and backgrounds compared with data for the observables used in the fiducial cross-section fit. The hatched bands represent combined statistical and systematic uncertainties, after propagating the constraints and correlations obtained from the fit to data. All background categories except single top and W +jets are combined in one category called Other bkg. The first and last bins contain underflow and overflow events, respectively.

band, is tested as follows. Pseudo-data are created by reweighting the detector-level prediction for events passing the selection to match the corresponding distribution in data in SR2, and the $t\bar{t}$ cross-section is extracted. No significant impact on the measured cross-section is observed.

Using the measured fiducial cross-section and the acceptance with its uncertainty from Table 2, and assuming that the uncertainties of the A_{fid} are not correlated with those obtained in the fit, the $t\bar{t}$ cross-section extrapolated to the full phase space is

$$\begin{aligned}\sigma_{\text{inc}}^{\text{ext}} &= 820 \pm 0.4 (\text{stat.}) \pm 37 (\text{syst.}) \pm 14 (\text{lumi.}) \text{ pb} \\ &= 820 \pm 40 \text{ pb}.\end{aligned}$$

The $t\bar{t}$ cross-section in the full phase space, referred to as inclusive cross-section, measured in the dedicated fit is

$$\begin{aligned}\sigma_{\text{inc}} &= 830 \pm 0.4 (\text{stat.}) \pm 36 (\text{syst.}) \pm 14 (\text{lumi.}) \text{ pb} \\ &= 830 \pm 38 \text{ pb}.\end{aligned}$$

The two results are compatible within the uncertainties and are in agreement with the theoretical NNLO + NNLL prediction for the top-quark mass of 172.5 GeV. The difference between the central values arises from the different assumptions related to the $t\bar{t}$ modelling uncertainties. For the inclusive measurement, the alternative models are assumed to have the same $\sigma_{t\bar{t}}$ in the full phase space, while for the fiducial measurement they are assumed to have the same cross-section after applying the fiducial selection. This results in different normalisation components of the signal modelling uncertainties, leading to different impacts of these uncertainties on the measured cross-section for the same post-fit values of the corresponding nuisance parameters.

The dependence of the measured inclusive $t\bar{t}$ cross-section on m_t is determined by repeating the fit to data after replacing the nominal input $t\bar{t}$ distributions by those from the samples generated with the same set-up as the nominal but with $m_t = 171, 172, 173$ and 174 GeV, assuming that the $t\bar{t}$ modelling uncertainties are independent of m_t . The dependence is found to be $1/\sigma_{\text{inc}} \times d\sigma_{\text{inc}}/dm_t = -1.7\%/GeV$.

Fig. 3 presents the ranking of the effects of different systematic uncertainties on the inclusive measurement. The impact of each NP, θ , is computed by comparing the nominal best-fit value of

σ_{inc} with the result of the fit when fixing the considered nuisance parameter to its best-fit value, $\hat{\theta}$, shifted by its pre-fit (post-fit) uncertainties $\pm\Delta\theta$ ($\pm\Delta\hat{\theta}$). The ranking plot shows that the uncertainty in σ_{inc} is dominated by the difference in the $t\bar{t}$ inclusive acceptance and the migration parameter between the nominal and the alternative parton shower and hadronisation model. The NP corresponding to the migration parameter is constrained, indicating that the normalisation effects of the alternative model vary significantly between the three regions. In SR1 (SR3), the alternative model predicts 1.4% (2.3%) larger yield while in SR2 it predicts 7.1% smaller yield than in the nominal $t\bar{t}$ simulation. These variations are much larger than the data uncertainty and allow the data to constrain this uncertainty. To check that this choice for the parameterisation of the parton shower systematic uncertainty does not affect the result, an alternative parameterisation is implemented with three normalisation and three shape NPs uncorrelated between three signal regions. No change in the central value or total uncertainty is observed, while the parameters show similar level of constraints and pulls as in the baseline fit. Other significant contributions to the uncertainty arise from the modelling of final-state radiation in SR1 and the top-quark p_T model. As expected, the latter is pulled towards the NNLO prediction, which is approximated here by a one-dimensional top-quark p_T reweighting. The uncertainty in the integrated luminosity is the highest-ranked experimental uncertainty.

A breakdown of the contributions from different categories of systematic uncertainties is presented in Table 3. The largest uncertainties, in both the fiducial and inclusive cross-section measurements, arise from the shower and hadronisation modelling and the scale variations. The source of the largest experimental uncertainty is the jet reconstruction category which includes uncertainties from jet identification, calibration, resolution and the JVT requirement.

Several tests were performed to check the stability of the result. To examine the disagreement between data and prediction observed in jet p_T spectra as illustrated in Fig. 2, the impact of changing the minimum jet p_T requirement was studied by repeating the analysis while selecting events with a minimum jet p_T of 30 GeV and 35 GeV instead of 25 GeV. In both cases, the measured cross-section changed by less than 2% and did not show a trend depending on the jet p_T cut.

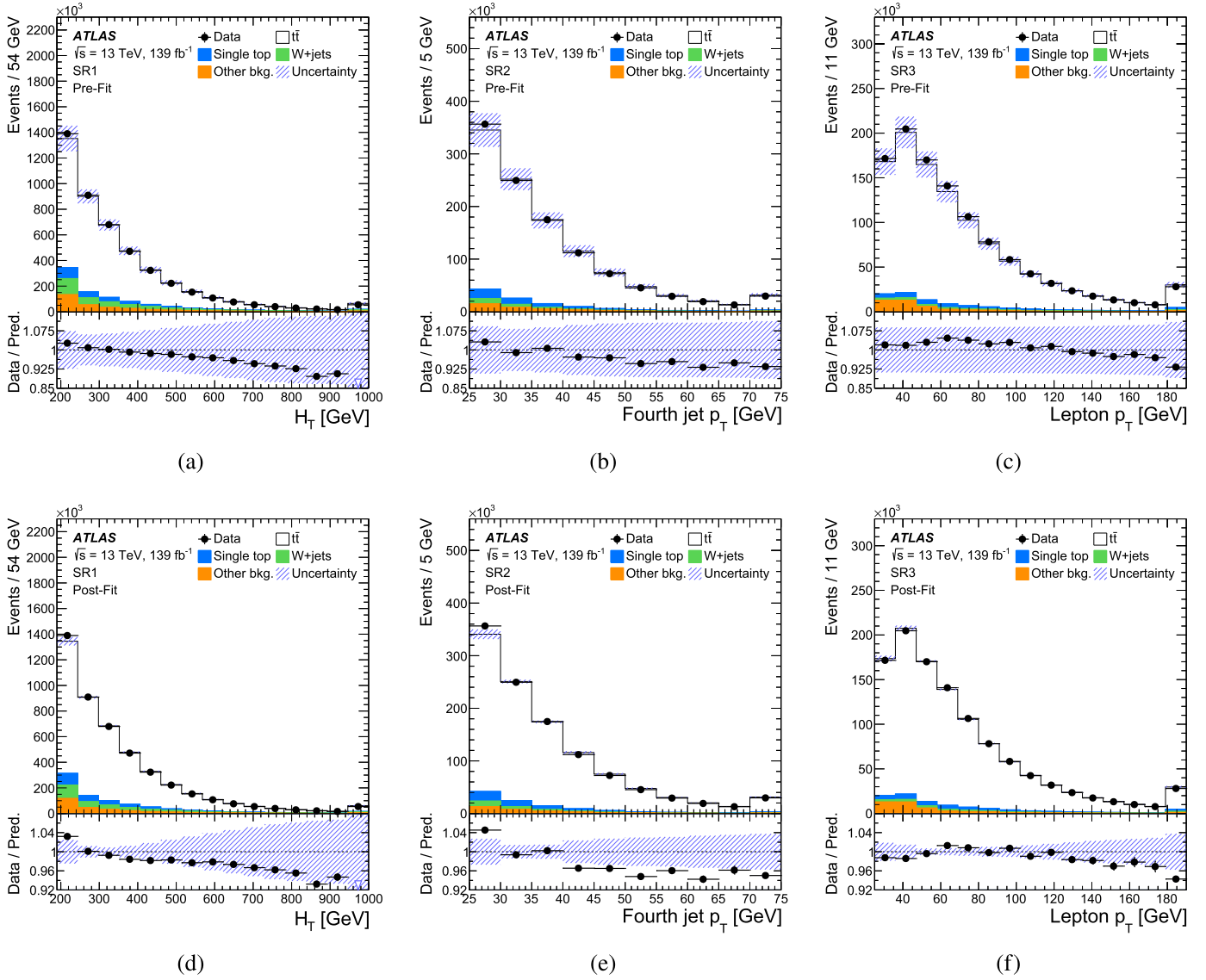


Fig. 2. Pre-fit (top) and post-fit (bottom) distributions of the scalar sum of jet transverse momenta in the event (H_T) in SR1 (left), the fourth largest jet p_T in SR2 (middle) and the lepton p_T in SR3 (right) for the fiducial cross-section measurement. The hatched bands represent combined statistical and systematic uncertainties. The first and last bins contain underflow and overflow events, respectively.

The approach to performing ME to parton shower matching differs between NLO generators and, in general, can be a source of uncertainty. However, it is not straightforward to separate the effect of the algorithmic difference in the implementation of such matching from other effects when replacing one ME generator by an alternative one, matched to the same parton shower. This may involve changes in the parameters of the parton shower that can lead to a much larger effect than the targeted one. For this reason, the effect of the generator choice is not included in the fit model. However, its impact on the result is checked by comparing two alternative $t\bar{t}$ samples generated with POWHEG-Box v2 and MADGRAPH5_aMC@NLO, both interfaced to HERWIG 7.1.3 [91]. A symmetrised difference between these two samples is applied as an additional systematic uncertainty, correlated between regions. No significant impact on the central value or the uncertainty is observed for either the inclusive or the fiducial measurements.

The stability of the result with respect to the choice of correlation scheme for the initial- and final-state radiation uncertainties, and for the μ_R and μ_F scale variations, was studied. In the alternative scheme, the uncertainties were treated as fully correlated

across the signal regions. No effect on either the measured cross-sections or the uncertainties was observed.

9. Conclusion

Measurements of the inclusive and fiducial $t\bar{t}$ production cross-sections are performed in the lepton+jets channel using proton-proton collision data at $\sqrt{s} = 13$ TeV recorded by the ATLAS detector at the LHC during 2015–2018, corresponding to an integrated luminosity of 139 fb^{-1} . The analysis is performed in three regions requiring different jet multiplicities and different numbers of b -tagged jets. The $t\bar{t}$ production cross-section and its uncertainty are extracted from a profile-likelihood fit to data of the distributions of discriminating variables in these three regions, assuming $m_t = 172.5$ GeV. The fiducial cross-section is measured with a precision of 4.3% to be $\sigma_{\text{fid}} = 110.7 \pm 4.8 \text{ pb} = 110.7 \pm 0.05 \text{ (stat.)}^{+4.5}_{-4.3} \text{ (syst.)} \pm 1.9 \text{ (lumi.) pb}$, and the inclusive cross-section is measured with a precision of 4.6% to be $\sigma_{\text{inc}} = 830 \pm 38 \text{ pb} = 830 \pm 0.4 \text{ (stat.)} \pm 36 \text{ (syst.)} \pm 14 \text{ (lumi.) pb}$. The inclusive result is in agreement with the theoretical NNLO + NNLL

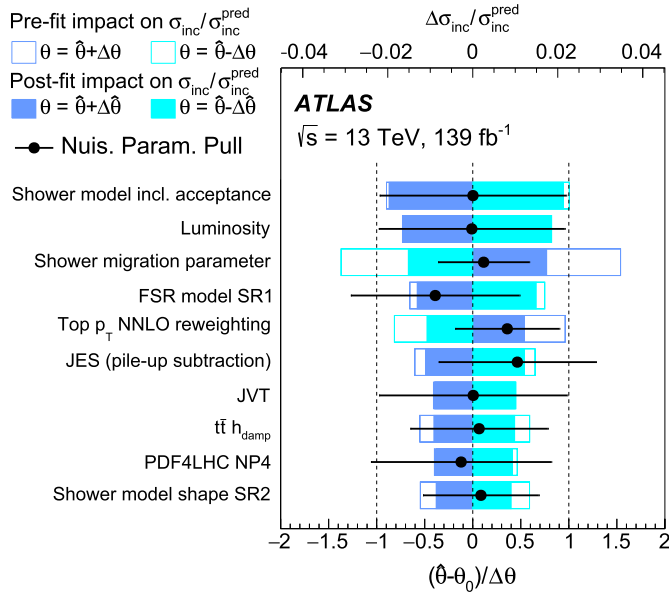


Fig. 3. Ranking plot showing the effect of the ten most important systematic uncertainties on the measured cross-section, normalised to the predicted value, in the inclusive fit to data. The impact of each NP, $\Delta\sigma_{\text{inc}}/\sigma_{\text{inc}}^{\text{pred}}$, is computed by comparing the nominal best-fit value of $\sigma_{\text{inc}}/\sigma_{\text{inc}}^{\text{pred}}$ with the result of the fit when fixing the considered nuisance parameter to its best-fit value, $\hat{\theta}$, shifted by its pre-fit and post-fit uncertainties $\pm\Delta\theta$ ($\pm\Delta\hat{\theta}$). The empty boxes show the pre-fit impact while the filled boxes show the post-fit impact of each nuisance parameter on the result. The black dots represent the post-fit value (pull) of each NP where the pre-fit value is subtracted, while the black line represents the post-fit uncertainty normalised to the pre-fit uncertainty. The “JES (pile-up subtraction)” is one of the 29 components of the JES uncertainty, the “FSR model SR1” is the FSR scale uncertainty in SR1 and the “PDF4LHC NP4” is one of the 30 independent PDF variations. Other components are described in Section 6.

Table 3

Impact of different categories of systematic uncertainties and data statistics on the fiducial and inclusive measurements. The quoted values are obtained by repeating the fit, fixing a set of nuisance parameters of the sources corresponding to the considered category, and subtracting in quadrature the resulting uncertainty from the total uncertainty of the nominal fit presented in the last line. The total uncertainty is different from the sum in quadrature of the different components due to correlations between nuisance parameters built by the fit. The categories are defined in Section 6.

Category	$\frac{\Delta\sigma_{\text{fid}}}{\sigma_{\text{fid}}} [\%]$	$\frac{\Delta\sigma_{\text{inc}}}{\sigma_{\text{inc}}} [\%]$
Signal modelling		
$t\bar{t}$ shower/hadronisation	± 2.8	± 2.9
$t\bar{t}$ scale variations	± 1.4	± 2.0
Top p_T NNLO reweighting	± 0.4	± 1.1
$t\bar{t}$ h_{damp}	± 1.5	± 1.4
$t\bar{t}$ PDF	± 1.4	± 1.5
Background modelling		
MC background modelling	± 1.8	± 2.0
Multijet background	± 0.8	± 0.6
Detector modelling		
Jet reconstruction	± 2.5	± 2.6
Luminosity	± 1.7	± 1.7
Flavour tagging	± 1.2	± 1.3
E_T^{miss} + pile-up	± 0.3	± 0.3
Muon reconstruction	± 0.6	± 0.5
Electron reconstruction	± 0.7	± 0.6
Simulation stat. uncertainty	± 0.6	± 0.7
Total systematic uncertainty		
Data statistical uncertainty	± 0.05	± 0.05
Total uncertainty	± 4.3	± 4.6

QCD calculation as well as with the ATLAS measurement in the electron–muon channel and with CMS measurements.

Declaration of competing interest

The authors declare that they have no known competing financial interests or personal relationships that could have appeared to influence the work reported in this paper.

Acknowledgements

We thank CERN for the very successful operation of the LHC, as well as the support staff from our institutions without whom ATLAS could not be operated efficiently.

We acknowledge the support of ANPCyT, Argentina; YerPhI, Armenia; ARC, Australia; BMWFW and FWF, Austria; ANAS, Azerbaijan; SSTC, Belarus; CNPq and FAPESP, Brazil; NSERC, NRC and CFI, Canada; CERN; CONICYT, Chile; CAS, MOST and NSFC, China; COLCIENCIAS, Colombia; MSMT CR, MPO CR and VSC CR, Czech Republic; DNRF and DNSRC, Denmark; IN2P3-CNRS and CEA-DRF/IRFU, France; SRNSFG, Georgia; BMBF, HGF and MPG, Germany; GSRT, Greece; RGC and Hong Kong SAR, China; ISF and Benoziyo Center, Israel; INFN, Italy; MEXT and JSPS, Japan; CNRST, Morocco; NWO, Netherlands; RCN, Norway; MNiSW and NCN, Poland; FCT, Portugal; MNE/IFA, Romania; MES of Russia and NRC KI, Russia Federation; JINR; MESTD, Serbia; MSSR, Slovakia; ARRS and MIZŠ, Slovenia; DST/NRF, South Africa; MINECO, Spain; SRC and Wallenberg Foundation, Sweden; SERI, SNSF and Cantons of Bern and Geneva, Switzerland; MOST, Taiwan; TAEK, Turkey; STFC, United Kingdom; DOE and NSF, United States of America. In addition, individual groups and members have received support from BCKDF, Canarie, Compute Canada and CRC, Canada; ERC, ERDF, Horizon 2020, Marie Skłodowska-Curie Actions and COST, European Union; Investissements d’Avenir Labex, Investissements d’Avenir Idex and ANR, France; DFG and AvH Foundation, Germany; Herakleitos, Thales and Aristeia programmes co-financed by EU-ESF and the Greek NSRF, Greece; BSF-NSF and GIF, Israel; CERCA Programme Generalitat de Catalunya and PROMETEO Programme Generalitat Valenciana, Spain; Göran Gustafssons Stiftelse, Sweden; The Royal Society and Leverhulme Trust, United Kingdom.

The crucial computing support from all WLCG partners is acknowledged gratefully, in particular from CERN, the ATLAS Tier-1 facilities at TRIUMF (Canada), NDGF (Denmark, Norway, Sweden), CC-IN2P3 (France), KIT/GridKA (Germany), INFN-CNAF (Italy), NL-T1 (Netherlands), PIC (Spain), ASGC (Taiwan), RAL (UK) and BNL (USA), the Tier-2 facilities worldwide and large non-WLCG resource providers. Major contributors of computing resources are listed in Ref. [92].

References

- [1] ATLAS Collaboration, Measurement of the top quark mass in the $t\bar{t} \rightarrow \text{lepton} + \text{jets}$ channel from $\sqrt{s} = 8$ TeV ATLAS data and combination with previous results, Eur. Phys. J. C 79 (2019) 290, arXiv:1810.01772 [hep-ex].
- [2] CMS Collaboration, Measurement of the top quark mass using proton–proton data at $\sqrt{s} = 7$ and 8 TeV, Phys. Rev. D 93 (2016) 072004, arXiv:1509.04044 [hep-ex].
- [3] A. Buckley, et al., Constraining top quark effective theory in the LHC Run II era, J. High Energy Phys. 04 (2016) 15, arXiv:1512.03360 [hep-ph].
- [4] M. Cacciari, M. Czakon, M. Mangano, A. Mitov, P. Nason, Top-pair production at hadron colliders with next-to-next-to-leading logarithmic soft-gluon resummation, Phys. Lett. B 710 (2012) 612, arXiv:1111.5869 [hep-ph].
- [5] P. Bärnreuther, M. Czakon, A. Mitov, Percent-level-precision physics at the Tevatron: next-to-next-to-leading order QCD corrections to $q\bar{q} \rightarrow t\bar{t} + X$, Phys. Rev. Lett. 109 (2012) 132001, arXiv:1204.5201 [hep-ph].
- [6] M. Czakon, A. Mitov, NNLO corrections to top-pair production at hadron colliders: the all-fermionic scattering channels, J. High Energy Phys. 12 (2012) 054, arXiv:1207.0236 [hep-ph].

- [7] M. Czakon, A. Mitov, NNLO corrections to top pair production at hadron colliders: the quark-gluon reaction, *J. High Energy Phys.* 01 (2013) 080, arXiv:1210.6832 [hep-ph].
- [8] M. Czakon, P. Fiedler, A. Mitov, Total top-quark pair-production cross section at hadron colliders through $O(\alpha_s^3)$, *Phys. Rev. Lett.* 110 (2013) 252004, arXiv:1303.6254 [hep-ph].
- [9] S. Catani, et al., Top-quark pair hadroproduction at next-to-next-to-leading order in QCD, *Phys. Rev. D* 99 (2019) 051501, arXiv:1901.04005 [hep-ph].
- [10] M. Czakon, A. Mitov, Top++: a program for the calculation of the top-pair cross-section at hadron colliders, *Comput. Phys. Commun.* 185 (2014) 2930, arXiv:1112.5675 [hep-ph].
- [11] A.D. Martin, W.J. Stirling, R.S. Thorne, G. Watt, Parton distributions for the LHC, *Eur. Phys. J. C* 63 (2009) 189, arXiv:0901.0002 [hep-ph].
- [12] A.D. Martin, W.J. Stirling, R.S. Thorne, G. Watt, Uncertainties on α_s in global PDF analyses and implications for predicted hadronic cross sections, *Eur. Phys. J. C* 64 (2009) 653, arXiv:0905.3531 [hep-ph].
- [13] M. Botje, et al., The PDF4LHC working group interim recommendations, arXiv:1101.0538 [hep-ph], 2011.
- [14] H.-L. Lai, et al., New parton distributions for collider physics, *Phys. Rev. D* 82 (2010) 074024, arXiv:1007.2241 [hep-ph].
- [15] J. Gao, et al., CT10 next-to-next-to-leading order global analysis of QCD, *Phys. Rev. D* 89 (2014) 033009, arXiv:1302.6246 [hep-ph].
- [16] R.D. Ball, et al., Parton distributions with LHC data, *Nucl. Phys. B* 867 (2013) 244, arXiv:1207.1303 [hep-ph].
- [17] ATLAS Collaboration, Measurement of the $t\bar{t}$ production cross-section using $e\mu$ events with b -tagged jets in pp collisions at $\sqrt{s} = 7$ and 8 TeV with the ATLAS detector, *Eur. Phys. J. C* 74 (2014) 3109, arXiv:1406.5375 [hep-ex], Addendum: *Eur. Phys. J. C* 76 (2016) 642.
- [18] ATLAS Collaboration, Measurement of the $t\bar{t}$ production cross section in the τ -jets final state in pp collisions at $\sqrt{s} = 8$ TeV using the ATLAS detector, *Phys. Rev. D* 95 (2017) 072003, arXiv:1702.08839 [hep-ex].
- [19] ATLAS Collaboration, Measurement of the $t\bar{t}$ production cross-section and lepton differential distributions in $e\mu$ dilepton events from pp collisions at $\sqrt{s} = 13$ TeV with the ATLAS detector, *Eur. Phys. J. C* 80 (2020) 528, arXiv:1910.08819 [hep-ex].
- [20] CMS Collaboration, Measurement of the $t\bar{t}$ production cross section in the $e\mu$ channel in proton-proton collisions at $\sqrt{s} = 7$ and 8 TeV, *J. High Energy Phys.* 08 (2016) 029, arXiv:1603.02303 [hep-ex].
- [21] CMS Collaboration, Measurements of the $t\bar{t}$ production cross section in lepton+jets final states in pp collisions at 8 TeV and ratio of 8 to 7 TeV cross sections, *Eur. Phys. J. C* 77 (2017) 15, arXiv:1602.09024 [hep-ex].
- [22] CMS Collaboration, Measurement of the $t\bar{t}$ production cross section using events in the $e\mu$ final state in pp collisions at $\sqrt{s} = 13$ TeV, *Eur. Phys. J. C* 77 (2017) 172, arXiv:1611.04040 [hep-ex].
- [23] CMS Collaboration, Measurement of the $t\bar{t}$ production cross section using events with one lepton and at least one jet in pp collisions at $\sqrt{s} = 13$ TeV, *J. High Energy Phys.* 09 (2017) 051, arXiv:1701.06228 [hep-ex].
- [24] CMS Collaboration, Measurement of the $t\bar{t}$ production cross section, the top quark mass, and the strong coupling constant using dilepton events in pp collisions at $\sqrt{s} = 13$ TeV, *Eur. Phys. J. C* 79 (2019) 368, arXiv:1812.10505 [hep-ex].
- [25] CMS Collaboration, Measurement of the inclusive $t\bar{t}$ cross section in pp collisions at $\sqrt{s} = 5.02$ TeV using final states with at least one charged lepton, *J. High Energy Phys.* 03 (2018) 115, arXiv:1711.03143 [hep-ex].
- [26] ATLAS Collaboration, Measurement of the $t\bar{t}$ production cross-section and lepton differential distributions in $e\mu$ dilepton events from pp collisions at $\sqrt{s} = 13$ TeV with the ATLAS detector, arXiv:1910.08819 [hep-ex], 2019.
- [27] ATLAS Collaboration, The ATLAS experiment at the CERN Large Hadron Collider, *J. Instrum.* 3 (2008) S08003.
- [28] B. Abbott, et al., Production and integration of the ATLAS Insertable B-Layer, *J. Instrum.* 13 (2018) T05008, arXiv:1803.00844 [physics.ins-det].
- [29] ATLAS Collaboration, ATLAS Insertable B-Layer technical design report addendum, CERN-LHCC-2012-009, Addendum to CERN-LHCC-2010-013, ATLAS-TDR-019, <https://cds.cern.ch/record/1451888>, 2012.
- [30] ATLAS Collaboration, Performance of the ATLAS trigger system in 2015, *Eur. Phys. J. C* 77 (2017) 317, arXiv:1611.09661 [hep-ex].
- [31] ATLAS Collaboration, ATLAS data quality operations and performance for 2015–2018 data-taking, *J. Instrum.* 15 (2020) P04003, arXiv:1911.04632 [physics.ins-det].
- [32] T. Sjöstrand, S. Mrenna, P. Skands, A brief introduction to PYTHIA 8.1, *Comput. Phys. Commun.* 178 (2008) 852, arXiv:0710.3820 [hep-ph].
- [33] ATLAS Collaboration, The Pythia 8 A3 tune description of ATLAS minimum bias and inelastic measurements incorporating the Donnachie–Landshoff diffractive model, ATL-PHYS-PUB-2016-017, <https://cds.cern.ch/record/2206965>, 2016.
- [34] S. Frixione, P. Nason, G. Ridolfi, A positive-weight next-to-leading-order Monte Carlo for heavy flavour hadroproduction, *J. High Energy Phys.* 09 (2007) 126, arXiv:0707.3088 [hep-ph].
- [35] S. Frixione, P. Nason, G. Ridolfi, The POWHEG-hvq manual version 1.0, arXiv:0707.3081 [hep-ph], 2007.
- [36] P. Nason, A new method for combining NLO QCD with shower Monte Carlo algorithms, *J. High Energy Phys.* 11 (2004) 040, arXiv:hep-ph/0409146.
- [37] S. Frixione, P. Nason, C. Oleari, Matching NLO QCD computations with parton shower simulations: the POWHEG method, *J. High Energy Phys.* 11 (2007) 070, arXiv:0709.2092 [hep-ph].
- [38] S. Alioli, P. Nason, C. Oleari, E. Re, A general framework for implementing NLO calculations in shower Monte Carlo programs: the POWHEG BOX, *J. High Energy Phys.* 06 (2010) 043, arXiv:1002.2581 [hep-ph].
- [39] R.D. Ball, et al., Parton distributions for the LHC Run II, *J. High Energy Phys.* 04 (2015) 040, arXiv:1410.8849 [hep-ph].
- [40] ATLAS Collaboration, Studies on top-quark Monte Carlo modelling for Top2016, ATL-PHYS-PUB-2016-020, <https://cds.cern.ch/record/2216168>, 2016.
- [41] T. Sjöstrand, et al., An introduction to PYTHIA 8.2, *Comput. Phys. Commun.* 191 (2015) 159, arXiv:1410.3012 [hep-ph].
- [42] ATLAS Collaboration, ATLAS Pythia 8 tunes to 7 TeV data, ATL-PHYS-PUB-2014-021, <https://cds.cern.ch/record/1966419>, 2014.
- [43] S. Frixione, E. Laenen, P. Motylinski, C.D. White, B.R. Webber, Single-top hadroproduction in association with a W boson, *J. High Energy Phys.* 07 (2008) 029, arXiv:0805.3067 [hep-ph].
- [44] E. Bothmann, et al., Event generation with Sherpa 2.2, *SciPost Phys.* 7 (2019) 034, arXiv:1905.09127 [hep-ph].
- [45] T. Gleisberg, S. Höche, Comix, a new matrix element generator, *J. High Energy Phys.* 12 (2008) 039, arXiv:0808.3674 [hep-ph].
- [46] F. Cascioli, P. Maierhöfer, S. Pozzorini, Scattering amplitudes with open loops, *Phys. Rev. Lett.* 108 (2012) 111601, arXiv:1111.5206 [hep-ph].
- [47] A. Denner, S. Dittmaier, L. Hofer, Collier: a fortran-based complex one-loop library in extended regularizations, *Comput. Phys. Commun.* 212 (2017) 220, arXiv:1604.06792 [hep-ph].
- [48] S. Schumann, F. Krauss, A parton shower algorithm based on Catani–Seymour dipole factorisation, *J. High Energy Phys.* 03 (2008) 038, arXiv:0709.1027 [hep-ph].
- [49] S. Höche, F. Krauss, M. Schönherr, F. Siegert, A critical appraisal of NLO + PS matching methods, *J. High Energy Phys.* 09 (2012) 049, arXiv:1111.1220 [hep-ph].
- [50] S. Höche, F. Krauss, M. Schönherr, F. Siegert, QCD matrix elements + parton showers. The NLO case, *J. High Energy Phys.* 04 (2013) 027, arXiv:1207.5030 [hep-ph].
- [51] S. Catani, F. Krauss, B.R. Webber, R. Kuhn, QCD matrix elements + parton showers, *J. High Energy Phys.* 11 (2001) 063, arXiv:hep-ph/0109231 [hep-ph].
- [52] S. Höche, F. Krauss, S. Schumann, F. Siegert, QCD matrix elements and truncated showers, *J. High Energy Phys.* 05 (2009) 053, arXiv:0903.1219 [hep-ph].
- [53] J. Alwall, et al., The automated computation of tree-level and next-to-leading order differential cross sections, and their matching to parton shower simulations, *J. High Energy Phys.* 07 (2014) 079, arXiv:1405.0301 [hep-ph].
- [54] D.J. Lange, The EvtGen particle decay simulation package, *Nucl. Instrum. Methods Phys. Res., Sect. A* 462 (2001) 152.
- [55] ATLAS Collaboration, The ATLAS simulation infrastructure, *Eur. Phys. J. C* 70 (2010) 823, arXiv:1005.4568 [physics.ins-det].
- [56] S. Agostinelli, et al., GEANT4 – a simulation toolkit, *Nucl. Instrum. Methods Phys. Res., Sect. A* 506 (2003) 250.
- [57] ATLAS Collaboration, Fast simulation for ATLAS: Atlfast-II and ISF, ATL-SOFT-PROC-2012-065, <http://cds.cern.ch/record/1458503>, 2012.
- [58] ATLAS Collaboration, Electron and photon performance measurements with the ATLAS detector using the 2015–2017 LHC proton-proton collision data, *J. Instrum.* 14 (2019) P12006, arXiv:1908.00005 [hep-ex].
- [59] ATLAS Collaboration, Muon reconstruction performance of the ATLAS detector in proton-proton collision data at $\sqrt{s} = 13$ TeV, *Eur. Phys. J. C* 76 (2016) 292, arXiv:1603.05598 [hep-ex].
- [60] ATLAS Collaboration, Vertex reconstruction performance of the ATLAS detector at $\sqrt{s} = 13$ TeV, ATL-PHYS-PUB-2015-026, <https://cds.cern.ch/record/2037717>, 2015.
- [61] ATLAS Collaboration, Topological cell clustering in the ATLAS calorimeters and its performance in LHC Run 1, *Eur. Phys. J. C* 77 (2017) 490, arXiv:1603.02934 [hep-ex].
- [62] M. Cacciari, G.P. Salam, G. Soyez, The anti- k_t jet clustering algorithm, *J. High Energy Phys.* 04 (2008) 063, arXiv:0802.1189 [hep-ph].
- [63] M. Cacciari, G.P. Salam, G. Soyez, Fastjet user manual, *Eur. Phys. J. C* 72 (2012) 1896, arXiv:1111.6097 [hep-ph].
- [64] ATLAS Collaboration, Jet energy scale measurements and their systematic uncertainties in proton-proton collisions at $\sqrt{s} = 13$ TeV with the ATLAS detector, *Phys. Rev. D* 96 (2017) 072002, arXiv:1703.09665 [hep-ex].
- [65] ATLAS Collaboration, Performance of pile-up mitigation techniques for jets in pp collisions at $\sqrt{s} = 8$ TeV using the ATLAS detector, *Eur. Phys. J. C* 76 (2016) 581, arXiv:1510.03823 [hep-ex].
- [66] ATLAS Collaboration, ATLAS b -jet identification performance and efficiency measurement with $t\bar{t}$ events in pp collisions at $\sqrt{s} = 13$ TeV, *Eur. Phys. J. C* 79 (2019) 970, arXiv:1907.05120 [hep-ex].
- [67] ATLAS Collaboration, Measurements of b -jet tagging efficiency with the ATLAS detector using $t\bar{t}$ events at $\sqrt{s} = 13$ TeV, *J. High Energy Phys.* 08 (2018) 089, arXiv:1805.01845 [hep-ex].
- [68] ATLAS Collaboration, Measurement of b -tagging efficiency of c -jets in $t\bar{t}$ events using a likelihood approach with the ATLAS detector, ATLAS-CONF-2018-001, <https://cds.cern.ch/record/2306649>, 2018.

- [69] ATLAS Collaboration, Calibration of light-flavour b -jet mistagging rates using ATLAS proton–proton collision data at $\sqrt{s} = 13$ TeV, ATLAS-CONF-2018-006, <https://cds.cern.ch/record/2314418>, 2018.
- [70] ATLAS Collaboration, Performance of missing transverse momentum reconstruction with the ATLAS detector using proton–proton collisions at $\sqrt{s} = 13$ TeV, Eur. Phys. J. C 78 (2018) 903, arXiv:1802.08168 [hep-ex].
- [71] ATLAS Collaboration, E_T^{miss} performance in the ATLAS detector using 2015–2016 LHC pp collisions, ATLAS-CONF-2018-023, <https://cds.cern.ch/record/2625233>, 2018.
- [72] ATLAS Collaboration, Measurements of top-quark pair differential and double-differential cross-sections in the ℓ +jets channel with pp collisions at $\sqrt{s} = 13$ TeV using the ATLAS detector, Eur. Phys. J. C 79 (2019) 1028, arXiv:1908.07305 [hep-ex].
- [73] ATLAS Collaboration, Measurement of the inclusive and fiducial $t\bar{t}$ production cross-sections in the lepton+jets channel in pp collisions at $\sqrt{s} = 8$ TeV with the ATLAS detector, Eur. Phys. J. C 78 (2018) 487, arXiv:1712.06857 [hep-ex].
- [74] D0 Collaboration, Measurement of the $t\bar{t}$ production cross section in $p\bar{p}$ collisions at $\sqrt{s} = 1.96$ -TeV using kinematic characteristics of lepton+jets events, Phys. Rev. D 76 (2007) 092007, arXiv:0705.2788 [hep-ex].
- [75] J.F. Donoghue, F.E. Low, S.-Y. Pi, Tensor analysis of hadronic jets in quantum chromodynamics, Phys. Rev. D 20 (1979) 2759.
- [76] G. Parisi, Super inclusive cross-sections, Phys. Lett. B 74 (1978) 65.
- [77] ATLAS Collaboration, Luminosity determination in pp collisions at $\sqrt{s} = 13$ TeV using the ATLAS detector at the LHC, ATLAS-CONF-2019-021, <https://cds.cern.ch/record/2677054>, 2019.
- [78] G. Avoni, et al., The new LUCID-2 detector for luminosity measurement and monitoring in ATLAS, J. Instrum. 13 (2018) P07017.
- [79] ATLAS Collaboration, Jet energy measurement with the ATLAS detector in proton–proton collisions at $\sqrt{s} = 7$ TeV, Eur. Phys. J. C 73 (2013) 2304, arXiv:1112.6426 [hep-ex].
- [80] M. Czakon, et al., Top-pair production at the LHC through NNLO QCD and NLO EW, J. High Energy Phys. 10 (2017) 186, arXiv:1705.04105 [hep-ph].
- [81] J. Bellm, et al., Herwig 7.0/Herwig++ 3.0 release note, Eur. Phys. J. C 76 (2016) 196, arXiv:1512.01178 [hep-ph].
- [82] M. Bahr, et al., Herwig++ physics and manual, Eur. Phys. J. C 58 (2008) 639, arXiv:0803.0883 [hep-ph].
- [83] L.A. Harland-Lang, A.D. Martin, P. Motylinski, R.S. Thorne, Parton distributions in the LHC era: MMHT2014 PDFs, Eur. Phys. J. C 75 (2015) 204, arXiv:1412.3989 [hep-ph].
- [84] ATLAS Collaboration, Improvements in $t\bar{t}$ modelling using NLO+PS Monte Carlo generators for Run 2, ATL-PHYS-PUB-2018-009, <https://cds.cern.ch/record/2630327>, 2018.
- [85] J. Butterworth, et al., PDF4LHC recommendations for LHC Run II, J. Phys. G 43 (2016) 023001, arXiv:1510.03865 [hep-ph].
- [86] N. Kidonakis, Next-to-next-to-next-to-leading-order soft-gluon corrections in hard-scattering processes near threshold, Phys. Rev. D 73 (2006) 034001, arXiv:hep-ph/0509079 [hep-ph].
- [87] E. Re, Single-top Wt-channel production matched with parton showers using the POWHEG method, Eur. Phys. J. C 71 (2011) 1547, arXiv:1009.2450 [hep-ph].
- [88] F. Krauss, Matrix elements and parton showers in hadronic interactions, J. High Energy Phys. 08 (2002) 015, arXiv:hep-ph/0205283 [hep-ph].
- [89] D. de Florian, et al., Handbook of LHC Higgs cross sections: 4. Deciphering the nature of the Higgs sector, arXiv:1610.07922 [hep-ph], 2016.
- [90] R. Barlow, C. Beeston, Fitting using finite Monte Carlo samples, Comput. Phys. Commun. 77 (1993) 219.
- [91] D. Reichelt, P. Richardson, A. Siodmok, Improving the simulation of quark and gluon jets with Herwig 7, Eur. Phys. J. C 77 (2017) 876, arXiv:1708.01491 [hep-ph].
- [92] ATLAS Collaboration, ATLAS computing acknowledgements, ATL-SOFT-PUB-2020-001, <https://cds.cern.ch/record/2717821>.

The ATLAS Collaboration

G. Aad¹⁰², B. Abbott¹²⁸, D.C. Abbott¹⁰³, A. Abed Abud³⁶, K. Abeling⁵³, D.K. Abhayasinghe⁹⁴, S.H. Abidi¹⁶⁶, O.S. AbouZeid⁴⁰, N.L. Abraham¹⁵⁵, H. Abramowicz¹⁶⁰, H. Abreu¹⁵⁹, Y. Abulaiti⁶, B.S. Acharya^{67a,67b,n}, B. Achkar⁵³, L. Adam¹⁰⁰, C. Adam Bourdarios⁵, L. Adamczyk^{84a}, L. Adamek¹⁶⁶, J. Adelman¹²¹, M. Adersberger¹¹⁴, A. Adiguzel^{12c}, S. Adorni⁵⁴, T. Adye¹⁴³, A.A. Affolder¹⁴⁵, Y. Afik¹⁵⁹, C. Agapopoulou⁶⁵, M.N. Agaras³⁸, A. Aggarwal¹¹⁹, C. Agheorghiesei^{27c}, J.A. Aguilar-Saavedra^{139f,139a,ad}, A. Ahmad³⁶, F. Ahmadov⁸⁰, W.S. Ahmed¹⁰⁴, X. Ai¹⁸, G. Aielli^{74a,74b}, S. Akatsuka⁸⁶, M. Akbiyik¹⁰⁰, T.P.A. Åkesson⁹⁷, E. Akilli⁵⁴, A.V. Akimov¹¹¹, K. Al Khoury⁶⁵, G.L. Alberghi^{23b,23a}, J. Albert¹⁷⁵, M.J. Alconada Verzini¹⁶⁰, S. Alderweireldt³⁶, M. Aleksa³⁶, I.N. Aleksandrov⁸⁰, C. Alexa^{27b}, T. Alexopoulos¹⁰, A. Alfonsi¹²⁰, F. Alfonsi^{23b,23a}, M. Alhroob¹²⁸, B. Ali¹⁴¹, S. Ali¹⁵⁷, M. Aliev¹⁶⁵, G. Alimonti^{69a}, C. Allaire³⁶, B.M.M. Allbrooke¹⁵⁵, B.W. Allen¹³¹, P.P. Allport²¹, A. Aloisio^{70a,70b}, F. Alonso⁸⁹, C. Alpigiani¹⁴⁷, E. Alunno Camelia^{74a,74b}, M. Alvarez Estevez⁹⁹, M.G. Alviggi^{70a,70b}, Y. Amaral Coutinho^{81b}, A. Ambler¹⁰⁴, L. Ambroz¹³⁴, C. Amelung²⁶, D. Amidei¹⁰⁶, S.P. Amor Dos Santos^{139a}, S. Amoroso⁴⁶, C.S. Amrouche⁵⁴, F. An⁷⁹, C. Anastopoulos¹⁴⁸, N. Andari¹⁴⁴, T. Andeen¹¹, J.K. Anders²⁰, S.Y. Andrean^{45a,45b}, A. Andreazza^{69a,69b}, V. Andrei^{61a}, C.R. Anelli¹⁷⁵, S. Angelidakis⁹, A. Angerami³⁹, A.V. Anisenkov^{122b,122a}, A. Annovi^{72a}, C. Antel⁵⁴, M.T. Anthony¹⁴⁸, E. Antipov¹²⁹, M. Antonelli⁵¹, D.J.A. Antrim¹⁷⁰, F. Anulli^{73a}, M. Aoki⁸², J.A. Aparisi Pozo¹⁷³, M.A. Aparo¹⁵⁵, L. Aperio Bella⁴⁶, N. Aranzabal Barrio³⁶, V. Araujo Ferraz^{81a}, R. Araujo Pereira^{81b}, C. Arcangeletti⁵¹, A.T.H. Arce⁴⁹, F.A. Arduh⁸⁹, J.-F. Arguin¹¹⁰, S. Argyropoulos⁵², J.-H. Arling⁴⁶, A.J. Armbruster³⁶, A. Armstrong¹⁷⁰, O. Arnaez¹⁶⁶, H. Arnold¹²⁰, Z.P. Arrubarrena Tame¹¹⁴, G. Artoni¹³⁴, H. Asada¹¹⁷, K. Asai¹²⁶, S. Asai¹⁶², T. Asawatavonvanich¹⁶⁴, N. Asbah⁵⁹, E.M. Asimakopoulou¹⁷¹, L. Asquith¹⁵⁵, J. Assahsah^{35d}, K. Assamagan²⁹, R. Astalos^{28a}, R.J. Atkin^{33a}, M. Atkinson¹⁷², N.B. Atlay¹⁹, H. Atmani⁶⁵, K. Augsten¹⁴¹, V.A. Austrup¹⁸¹, G. Avolio³⁶, M.K. Ayoub^{15a}, G. Azuelos^{110,al}, H. Bachacou¹⁴⁴, K. Bachas¹⁶¹, M. Backes¹³⁴, F. Backman^{45a,45b}, P. Bagnaia^{73a,73b}, M. Bahmani⁸⁵, H. Bahrasemani¹⁵¹, A.J. Bailey¹⁷³, V.R. Bailey¹⁷², J.T. Baines¹⁴³, C. Bakalis¹⁰, O.K. Baker¹⁸², P.J. Bakker¹²⁰, E. Bakos¹⁶, D. Bakshi Gupta⁸, S. Balaji¹⁵⁶, R. Balasubramanian¹²⁰, E.M. Baldin^{122b,122a}, P. Balek¹⁷⁹, F. Balli¹⁴⁴, W.K. Balunas¹³⁴, J. Balz¹⁰⁰, E. Banas⁸⁵, M. Bandieramonte¹³⁸, A. Bandyopadhyay²⁴, Sw. Banerjee^{180,i}, L. Barak¹⁶⁰, W.M. Barbe³⁸, E.L. Barberio¹⁰⁵, D. Barberis^{55b,55a}, M. Barbero¹⁰², G. Barbour⁹⁵, T. Barillari¹¹⁵, M.-S. Barisits³⁶, J. Barkeloo¹³¹, T. Barklow¹⁵², R. Barnea¹⁵⁹, B.M. Barnett¹⁴³, R.M. Barnett¹⁸, Z. Barnovska-Blenessy^{60a}, A. Baroncelli^{60a}, G. Barone²⁹, A.J. Barr¹³⁴,

L. Barranco Navarro^{45a,45b}, F. Barreiro⁹⁹, J. Barreiro Guimarães da Costa^{15a}, U. Barron¹⁶⁰, S. Barsov¹³⁷, F. Bartels^{61a}, R. Bartoldus¹⁵², G. Bartolini¹⁰², A.E. Barton⁹⁰, P. Bartos^{28a}, A. Basalaev⁴⁶, A. Basan¹⁰⁰, A. Bassalat^{65,ai}, M.J. Basso¹⁶⁶, R.L. Bates⁵⁷, S. Batlamous^{35e}, J.R. Batley³², B. Batool¹⁵⁰, M. Battaglia¹⁴⁵, M. Bause^{73a,73b}, F. Bauer¹⁴⁴, P. Bauer²⁴, H.S. Bawa³¹, A. Bayirli^{12c}, J.B. Beacham⁴⁹, T. Beau¹³⁵, P.H. Beauchemin¹⁶⁹, F. Becherer⁵², P. Bechtel²⁴, H.C. Beck⁵³, H.P. Beck^{20,p}, K. Becker¹⁷⁷, C. Becot⁴⁶, A. Beddall^{12d}, A.J. Beddall^{12a}, V.A. Bednyakov⁸⁰, M. Bedognetti¹²⁰, C.P. Bee¹⁵⁴, T.A. Beermann¹⁸¹, M. Begalli^{81b}, M. Begel²⁹, A. Behera¹⁵⁴, J.K. Behr⁴⁶, F. Beisiegel²⁴, M. Belfkir⁵, A.S. Bell⁹⁵, G. Bella¹⁶⁰, L. Bellagamba^{23b}, A. Bellerive³⁴, P. Bellos⁹, K. Beloborodov^{122b,122a}, K. Belotskiy¹¹², N.L. Belyaev¹¹², D. Benchekroun^{35a}, N. Benekos¹⁰, Y. Benhammou¹⁶⁰, D.P. Benjamin⁶, M. Benoit²⁹, J.R. Bensinger²⁶, S. Bentvelsen¹²⁰, L. Beresford¹³⁴, M. Beretta⁵¹, D. Berge¹⁹, E. Bergeaas Kuutmann¹⁷¹, N. Berger⁵, B. Bergmann¹⁴¹, L.J. Bergsten²⁶, J. Beringer¹⁸, S. Berlendis⁷, G. Bernardi¹³⁵, C. Bernius¹⁵², F.U. Bernlochner²⁴, T. Berry⁹⁴, P. Berta¹⁰⁰, A. Berthold⁴⁸, I.A. Bertram⁹⁰, O. Bessidskaia Bylund¹⁸¹, N. Besson¹⁴⁴, A. Bethani¹⁰¹, S. Bethke¹¹⁵, A. Betti⁴², A.J. Bevan⁹³, J. Beyer¹¹⁵, D.S. Bhattacharya¹⁷⁶, P. Bhattarai²⁶, V.S. Bhopatkar⁶, R. Bi¹³⁸, R.M. Bianchi¹³⁸, O. Biebel¹¹⁴, D. Biedermann¹⁹, R. Bielski³⁶, K. Bierwagen¹⁰⁰, N.V. Biesuz^{72a,72b}, M. Biglietti^{75a}, T.R.V. Billoud¹⁴¹, M. Bindi⁵³, A. Bingul^{12d}, C. Bini^{73a,73b}, S. Biondi^{23b,23a}, C.J. Birch-sykes¹⁰¹, M. Birman¹⁷⁹, T. Bisanz⁵³, J.P. Biswal³, D. Biswas^{180,i}, A. Bitadze¹⁰¹, C. Bittrich⁴⁸, K. Bjørke¹³³, T. Blazek^{28a}, I. Bloch⁴⁶, C. Blocker²⁶, A. Blue⁵⁷, U. Blumenschein⁹³, G.J. Bobbink¹²⁰, V.S. Bobrovnikov^{122b,122a}, S.S. Bocchetta⁹⁷, D. Boerner⁴⁶, D. Bogavac¹⁴, A.G. Bogdanchikov^{122b,122a}, C. Bohm^{45a}, V. Boisvert⁹⁴, P. Bokan^{171,53}, T. Bold^{84a}, A.E. Bolz^{61b}, M. Bomben¹³⁵, M. Bona⁹³, J.S. Bonilla¹³¹, M. Boonekamp¹⁴⁴, C.D. Booth⁹⁴, A.G. Borbély⁵⁷, H.M. Borecka-Bielska⁹¹, L.S. Borgna⁹⁵, A. Borisov¹²³, G. Borissov⁹⁰, D. Bortoletto¹³⁴, D. Boscherini^{23b}, M. Bosman¹⁴, J.D. Bossio Sola¹⁰⁴, K. Bouaouda^{35a}, J. Boudreau¹³⁸, E.V. Bouhova-Thacker⁹⁰, D. Boumediene³⁸, A. Boveia¹²⁷, J. Boyd³⁶, D. Boye^{33c}, I.R. Boyko⁸⁰, A.J. Bozson⁹⁴, J. Bracinik²¹, N. Brahimi^{60d}, G. Brandt¹⁸¹, O. Brandt³², F. Braren⁴⁶, B. Brau¹⁰³, J.E. Brau¹³¹, W.D. Breaden Madden⁵⁷, K. Brendlinger⁴⁶, R. Brenner¹⁵⁹, L. Brenner³⁶, R. Brenner¹⁷¹, S. Bressler¹⁷⁹, B. Brickwedde¹⁰⁰, D.L. Briglin²¹, D. Britton⁵⁷, D. Britzger¹¹⁵, I. Brock²⁴, R. Brock¹⁰⁷, G. Brooijmans³⁹, W.K. Brooks^{146d}, E. Brost²⁹, P.A. Bruckman de Renstrom⁸⁵, B. Brüers⁴⁶, D. Bruncko^{28b}, A. Bruni^{23b}, G. Bruni^{23b}, M. Bruschi^{23b}, N. Bruscino^{73a,73b}, L. Bryngemark¹⁵², T. Buanes¹⁷, Q. Buat¹⁵⁴, P. Buchholz¹⁵⁰, A.G. Buckley⁵⁷, I.A. Budagov⁸⁰, M.K. Bugge¹³³, F. Bühner⁵², O. Bulekov¹¹², B.A. Bullard⁵⁹, T.J. Burch¹²¹, S. Burdin⁹¹, C.D. Burgard¹²⁰, A.M. Burger¹²⁹, B. Burghgrave⁸, J.T.P. Burr⁴⁶, C.D. Burton¹¹, J.C. Burzynski¹⁰³, V. Büscher¹⁰⁰, E. Buschmann⁵³, P.J. Bussey⁵⁷, J.M. Butler²⁵, C.M. Buttar⁵⁷, J.M. Butterworth⁹⁵, P. Butti³⁶, W. Buttinger³⁶, C.J. Buxo Vazquez¹⁰⁷, A. Buzatu¹⁵⁷, A.R. Buzykaev^{122b,122a}, G. Cabras^{23b,23a}, S. Cabrera Urbán¹⁷³, D. Caforio⁵⁶, H. Cai¹³⁸, V.M.M. Cairo¹⁵², O. Cakir^{4a}, N. Calace³⁶, P. Calafiura¹⁸, G. Calderini¹³⁵, P. Calfayan⁶⁶, G. Callea⁵⁷, L.P. Caloba^{81b}, A. Caltabiano^{74a,74b}, S. Calvente Lopez⁹⁹, D. Calvet³⁸, S. Calvet³⁸, T.P. Calvet¹⁰², M. Calvetti^{72a,72b}, R. Camacho Toro¹³⁵, S. Camarda³⁶, D. Camarero Munoz⁹⁹, P. Camarri^{74a,74b}, M.T. Camerlingo^{75a,75b}, D. Cameron¹³³, C. Camincher³⁶, S. Campana³⁶, M. Campanelli⁹⁵, A. Camplani⁴⁰, V. Canale^{70a,70b}, A. Canesse¹⁰⁴, M. Cano Bret⁷⁸, J. Cantero¹²⁹, T. Cao¹⁶⁰, Y. Cao¹⁷², M.D.M. Capeans Garrido³⁶, M. Capua^{41b,41a}, R. Cardarelli^{74a}, F. Cardillo¹⁴⁸, G. Carducci^{41b,41a}, I. Carli¹⁴², T. Carli³⁶, G. Carlino^{70a}, B.T. Carlson¹³⁸, E.M. Carlson^{175,167a}, L. Carminati^{69a,69b}, R.M.D. Carney¹⁵², S. Caron¹¹⁹, E. Carquin^{146d}, S. Carrá⁴⁶, G. Carratta^{23b,23a}, J.W.S. Carter¹⁶⁶, T.M. Carter⁵⁰, M.P. Casado^{14,f}, A.F. Casha¹⁶⁶, E.G. Castiglia¹⁸², F.L. Castillo¹⁷³, L. Castillo Garcia¹⁴, V. Castillo Gimenez¹⁷³, N.F. Castro^{139a,139e}, A. Catinaccio³⁶, J.R. Catmore¹³³, A. Cattai³⁶, V. Cavaliere²⁹, V. Cavasinni^{72a,72b}, E. Celebi^{12b}, F. Celli¹³⁴, K. Cerny¹³⁰, A.S. Cerqueira^{81a}, A. Cerri¹⁵⁵, L. Cerrito^{74a,74b}, F. Cerutti¹⁸, A. Cervelli^{23b,23a}, S.A. Cetin^{12b}, Z. Chadi^{35a}, D. Chakraborty¹²¹, J. Chan¹⁸⁰, W.S. Chan¹²⁰, W.Y. Chan⁹¹, J.D. Chapman³², B. Chargeishvili^{158b}, D.G. Charlton²¹, T.P. Charman⁹³, M. Chatterjee²⁰, C.C. Chau³⁴, S. Che¹²⁷, S. Chekanov⁶, S.V. Chekulaev^{167a}, G.A. Chelkov^{80,ag}, B. Chen⁷⁹, C. Chen^{60a}, C.H. Chen⁷⁹, H. Chen^{15c}, H. Chen²⁹, J. Chen^{60a}, J. Chen³⁹, J. Chen²⁶, S. Chen¹³⁶, S.J. Chen^{15c}, X. Chen^{15b}, Y. Chen^{60a}, Y.-H. Chen⁴⁶, H.C. Cheng^{63a}, H.J. Cheng^{15a}, A. Cheplakov⁸⁰, E. Cheremushkina¹²³, R. Cherkaoui El Moursli^{35e}, E. Cheu⁷, K. Cheung⁶⁴, T.J.A. Chevaléras¹⁴⁴, L. Chevalier¹⁴⁴, V. Chiarella⁵¹, G. Chiarelli^{72a}, G. Chiodini^{68a}, A.S. Chisholm²¹, A. Chitan^{27b}, I. Chiu¹⁶², Y.H. Chiu¹⁷⁵, M.V. Chizhov⁸⁰, K. Choi¹¹, A.R. Chomont^{73a,73b}, Y.S. Chow¹²⁰, L.D. Christopher^{33e}, M.C. Chu^{63a}, X. Chu^{15a,15d}, J. Chudoba¹⁴⁰, J.J. Chwastowski⁸⁵, L. Chytka¹³⁰, D. Cieri¹¹⁵, K.M. Ciesla⁸⁵, V. Cindro⁹², I.A. Cioară^{27b},

A. Ciochio¹⁸, F. Ciotto^{70a,70b}, Z.H. Citron^{179,j}, M. Citterio^{69a}, D.A. Ciubotaru^{27b}, B.M. Ciungu¹⁶⁶, A. Clark⁵⁴, M.R. Clark³⁹, P.J. Clark⁵⁰, S.E. Clawson¹⁰¹, C. Clement^{45a,45b}, Y. Coadou¹⁰², M. Cobal^{67a,67c}, A. Coccaro^{55b}, J. Cochran⁷⁹, R. Coelho Lopes De Sa¹⁰³, H. Cohen¹⁶⁰, A.E.C. Coimbra³⁶, B. Cole³⁹, A.P. Colijn¹²⁰, J. Collot⁵⁸, P. Conde Muiño^{139a,139h}, S.H. Connell^{33c}, I.A. Connelly⁵⁷, S. Constantinescu^{27b}, F. Conventi^{70a,am}, A.M. Cooper-Sarkar¹³⁴, F. Cormier¹⁷⁴, K.J.R. Cormier¹⁶⁶, L.D. Corpe⁹⁵, M. Corradi^{73a,73b}, E.E. Corrigan⁹⁷, F. Corriveau^{104,ab}, M.J. Costa¹⁷³, F. Costanza⁵, D. Costanzo¹⁴⁸, G. Cowan⁹⁴, J.W. Cowley³², J. Crane¹⁰¹, K. Cranmer¹²⁵, R.A. Creager¹³⁶, S. Crépé-Renaudin⁵⁸, F. Crescioli¹³⁵, M. Cristinziani²⁴, V. Croft¹⁶⁹, G. Crosetti^{41b,41a}, A. Cueto⁵, T. Cuhadar Donszelmann¹⁷⁰, H. Cui^{15a,15d}, A.R. Cukierman¹⁵², W.R. Cunningham⁵⁷, S. Czekierda⁸⁵, P. Czodrowski³⁶, M.M. Czurylo^{61b}, M.J. Da Cunha Sargedas De Sousa^{60b}, J.V. Da Fonseca Pinto^{81b}, C. Da Via¹⁰¹, W. Dabrowski^{84a}, F. Dachs³⁶, T. Dado⁴⁷, S. Dahbi^{33e}, T. Dai¹⁰⁶, C. Dallapiccola¹⁰³, M. Dam⁴⁰, G. D'amen²⁹, V. D'Amico^{75a,75b}, J. Damp¹⁰⁰, J.R. Dandoy¹³⁶, M.F. Daneri³⁰, M. Danninger¹⁵¹, V. Dao³⁶, G. Darbo^{55b}, O. Dartsis⁵, A. Dattagupta¹³¹, T. Daubney⁴⁶, S. D'Auria^{69a,69b}, C. David^{167b}, T. Davidek¹⁴², D.R. Davis⁴⁹, I. Dawson¹⁴⁸, K. De⁸, R. De Asmundis^{70a}, M. De Beurs¹²⁰, S. De Castro^{23b,23a}, N. De Groot¹¹⁹, P. de Jong¹²⁰, H. De la Torre¹⁰⁷, A. De Maria^{15c}, D. De Pedis^{73a}, A. De Salvo^{73a}, U. De Sanctis^{74a,74b}, M. De Santis^{74a,74b}, A. De Santo¹⁵⁵, J.B. De Vivie De Regie⁶⁵, D.V. Dedovich⁸⁰, A.M. Deiana⁴², J. Del Peso⁹⁹, Y. Delabat Diaz⁴⁶, D. Delgove⁶⁵, F. Deliot¹⁴⁴, C.M. Delitzsch⁷, M. Della Pietra^{70a,70b}, D. Della Volpe⁵⁴, A. Dell'Acqua³⁶, L. Dell'Asta^{74a,74b}, M. Delmastro⁵, C. Delporte⁶⁵, P.A. Delsart⁵⁸, D.A. DeMarco¹⁶⁶, S. Demers¹⁸², M. Demichev⁸⁰, G. Demontigny¹¹⁰, S.P. Denisov¹²³, L. D'Eramo¹²¹, D. Derendarz⁸⁵, J.E. Derkaoui^{35d}, F. Derue¹³⁵, P. Dervan⁹¹, K. Desch²⁴, K. Dette¹⁶⁶, C. Deutsch²⁴, M.R. Devesa³⁰, P.O. Deviveiros³⁶, F.A. Di Bello^{73a,73b}, A. Di Ciaccio^{74a,74b}, L. Di Ciaccio⁵, W.K. Di Clemente¹³⁶, C. Di Donato^{70a,70b}, A. Di Girolamo³⁶, G. Di Gregorio^{72a,72b}, B. Di Micco^{75a,75b}, R. Di Nardo^{75a,75b}, K.F. Di Petrillo⁵⁹, R. Di Sipio¹⁶⁶, C. Diaconu¹⁰², F.A. Dias¹²⁰, T. Dias Do Vale^{139a}, M.A. Diaz^{146a}, F.G. Diaz Capriles²⁴, J. Dickinson¹⁸, M. Didenko¹⁶⁵, E.B. Diehl¹⁰⁶, J. Dietrich¹⁹, S. Díez Cornell⁴⁶, C. Díez Pardo¹⁵⁰, A. Dimitrievska¹⁸, W. Ding^{15b}, J. Dingfelder²⁴, S.J. Dittmeier^{61b}, F. Dittus³⁶, F. Djama¹⁰², T. Djobava^{158b}, J.I. Djuvsland¹⁷, M.A.B. Do Vale^{81c}, M. Dobre^{27b}, D. Dodsworth²⁶, C. Doglioni⁹⁷, J. Dolejsi¹⁴², Z. Dolezal¹⁴², M. Donadelli^{81d}, B. Dong^{60c}, J. Donini³⁸, A. D'Onofrio^{15c}, M. D'Onofrio⁹¹, J. Dopke¹⁴³, A. Doria^{70a}, M.T. Dova⁸⁹, A.T. Doyle⁵⁷, E. Drechsler¹⁵¹, E. Dreyer¹⁵¹, T. Dreyer⁵³, A.S. Drobac¹⁶⁹, D. Du^{60b}, T.A. du Pree¹²⁰, Y. Duan^{60d}, F. Dubinin¹¹¹, M. Dubovsky^{28a}, A. Dubreuil⁵⁴, E. Duchovni¹⁷⁹, G. Duckeck¹¹⁴, O.A. Ducu³⁶, D. Duda¹¹⁵, A. Dudarev³⁶, A.C. Dudder¹⁰⁰, E.M. Duffield¹⁸, M. D'uffizi¹⁰¹, L. Duflot⁶⁵, M. Dührssen³⁶, C. Dülse¹⁸¹, M. Dumancic¹⁷⁹, A.E. Dumitriu^{27b}, M. Dunford^{61a}, A. Duperrin¹⁰², H. Duran Yildiz^{4a}, M. Düren⁵⁶, A. Durglishvili^{158b}, D. Duschinger⁴⁸, B. Dutta⁴⁶, D. Duvnjak¹, G.I. Dyckes¹³⁶, M. Dyndal³⁶, S. Dysch¹⁰¹, B.S. Dziedzic⁸⁵, M.G. Eggleston⁴⁹, T. Eifert⁸, G. Eigen¹⁷, K. Einsweiler¹⁸, T. Ekelof¹⁷¹, H. El Jarrari^{35e}, V. Ellajosyula¹⁷¹, M. Ellert¹⁷¹, F. Ellinghaus¹⁸¹, A.A. Elliot⁹³, N. Ellis³⁶, J. Elmsheuser²⁹, M. Elsing³⁶, D. Emelianov¹⁴³, A. Emerman³⁹, Y. Enari¹⁶², M.B. Epland⁴⁹, J. Erdmann⁴⁷, A. Ereditato²⁰, P.A. Erland⁸⁵, M. Errenst¹⁸¹, M. Escalier⁶⁵, C. Escobar¹⁷³, O. Estrada Pastor¹⁷³, E. Etzion¹⁶⁰, H. Evans⁶⁶, M.O. Evans¹⁵⁵, A. Ezhilov¹³⁷, F. Fabbri⁵⁷, L. Fabbri^{23b,23a}, V. Fabiani¹¹⁹, G. Facini¹⁷⁷, R.M. Fakhruddinov¹²³, S. Falciano^{73a}, P.J. Falke²⁴, S. Falke³⁶, J. Faltova¹⁴², Y. Fang^{15a}, Y. Fang^{15a}, G. Fanourakis⁴⁴, M. Fanti^{69a,69b}, M. Faraj^{67a,67c}, A. Farbin⁸, A. Farilla^{75a}, E.M. Farina^{71a,71b}, T. Farooque¹⁰⁷, S.M. Farrington⁵⁰, P. Farthouat³⁶, F. Fassi^{35e}, P. Fassnacht³⁶, D. Fassouliotis⁹, M. Fauci Giannelli⁵⁰, W.J. Fawcett³², L. Fayard⁶⁵, O.L. Fedin^{137,o}, W. Fedorko¹⁷⁴, A. Fehr²⁰, M. Feickert¹⁷², L. Felgioni¹⁰², A. Fell¹⁴⁸, C. Feng^{60b}, M. Feng⁴⁹, M.J. Fenton¹⁷⁰, A.B. Fenyuk¹²³, S.W. Ferguson⁴³, J. Ferrando⁴⁶, A. Ferrante¹⁷², A. Ferrari¹⁷¹, P. Ferrari¹²⁰, R. Ferrari^{71a}, D.E. Ferreira de Lima^{61b}, A. Ferrer¹⁷³, D. Ferrere⁵⁴, C. Ferretti¹⁰⁶, F. Fiedler¹⁰⁰, A. Filipčič⁹², F. Filthaut¹¹⁹, K.D. Finelli²⁵, M.C.N. Fiolhais^{139a,139c,a}, L. Fiorini¹⁷³, F. Fischer¹¹⁴, J. Fischer¹⁰⁰, W.C. Fisher¹⁰⁷, T. Fitschen²¹, I. Fleck¹⁵⁰, P. Fleischmann¹⁰⁶, T. Flick¹⁸¹, B.M. Flierl¹¹⁴, L. Flores¹³⁶, L.R. Flores Castillo^{63a}, F.M. Follega^{76a,76b}, N. Fomin¹⁷, J.H. Foo¹⁶⁶, G.T. Forcolin^{76a,76b}, B.C. Forland⁶⁶, A. Formica¹⁴⁴, F.A. Förster¹⁴, A.C. Forti¹⁰¹, E. Fortin¹⁰², M.G. Foti¹³⁴, D. Fournier⁶⁵, H. Fox⁹⁰, P. Francavilla^{72a,72b}, S. Francescato^{73a,73b}, M. Franchini^{23b,23a}, S. Franchino^{61a}, D. Francis³⁶, L. Franco⁵, L. Franconi²⁰, M. Franklin⁵⁹, G. Frattari^{73a,73b}, A.N. Fray⁹³, P.M. Freeman²¹, B. Freund¹¹⁰, W.S. Freund^{81b}, E.M. Freundlich⁴⁷, D.C. Frizzell¹²⁸, D. Froidevaux³⁶, J.A. Frost¹³⁴, M. Fujimoto¹²⁶, C. Fukunaga¹⁶³, E. Fullana Torregrosa¹⁷³, T. Fusayasu¹¹⁶, J. Fuster¹⁷³, A. Gabrielli^{23b,23a}, A. Gabrielli³⁶,

S. Gadatsch⁵⁴, P. Gadow¹¹⁵, G. Gagliardi^{55b,55a}, L.G. Gagnon¹¹⁰, G.E. Gallardo¹³⁴, E.J. Gallas¹³⁴, B.J. Gallop¹⁴³, R. Gamboa Goni⁹³, K.K. Gan¹²⁷, S. Ganguly¹⁷⁹, J. Gao^{60a}, Y. Gao⁵⁰, Y.S. Gao^{31,l}, F.M. Garay Walls^{146a}, C. García¹⁷³, J.E. García Navarro¹⁷³, J.A. García Pascual^{15a}, C. Garcia-Argos⁵², M. Garcia-Sciveres¹⁸, R.W. Gardner³⁷, N. Garelli¹⁵², S. Gargiulo⁵², C.A. Garner¹⁶⁶, V. Garonne¹³³, S.J. Gasiorowski¹⁴⁷, P. Gaspar^{81b}, A. Gaudiello^{55b,55a}, G. Gaudio^{71a}, P. Gauzzi^{73a,73b}, I.L. Gavrilenko¹¹¹, A. Gavriluk¹²⁴, C. Gay¹⁷⁴, G. Gaycken⁴⁶, E.N. Gazis¹⁰, A.A. Geanta^{27b}, C.M. Gee¹⁴⁵, C.N.P. Gee¹⁴³, J. Geisen⁹⁷, M. Geisen¹⁰⁰, C. Gemme^{55b}, M.H. Genest⁵⁸, C. Geng¹⁰⁶, S. Gentile^{73a,73b}, S. George⁹⁴, T. Geralis⁴⁴, L.O. Gerlach⁵³, P. Gessinger-Befurt¹⁰⁰, G. Gessner⁴⁷, S. Ghasemi¹⁵⁰, M. Ghasemi Bostanabad¹⁷⁵, M. Ghneimat¹⁵⁰, A. Ghosh⁶⁵, A. Ghosh⁷⁸, B. Giacobbe^{23b}, S. Giagu^{73a,73b}, N. Giangiacomi^{23b,23a}, P. Giannetti^{72a}, A. Giannini^{70a,70b}, G. Giannini¹⁴, S.M. Gibson⁹⁴, M. Gignac¹⁴⁵, D.T. Gil^{84b}, B.J. Gilbert³⁹, D. Gillberg³⁴, G. Gilles¹⁸¹, D.M. Gingrich^{3,al}, M.P. Giordani^{67a,67c}, P.F. Giraud¹⁴⁴, G. Giudliarelli^{67a,67c}, D. Giugni^{69a}, F. Giuli^{74a,74b}, S. Gkaitatzis¹⁶¹, I. Gkialas^{9,g}, E.L. Gkougkousis¹⁴, P. Gkoutoumis¹⁰, L.K. Gladilin¹¹³, C. Glasman⁹⁹, J. Glatzer¹⁴, P.C.F. Glaysher⁴⁶, A. Glazov⁴⁶, G.R. Gledhill¹³¹, I. Gnesi^{41b,b}, M. Goblirsch-Kolb²⁶, D. Godin¹¹⁰, S. Goldfarb¹⁰⁵, T. Golling⁵⁴, D. Golubkov¹²³, A. Gomes^{139a,139b}, R. Goncalves Gama⁵³, R. Gonçalves^{139a,139c}, G. Gonella¹³¹, L. Gonella²¹, A. Gongadze⁸⁰, F. Gonnella²¹, J.L. Gonski³⁹, S. González de la Hoz¹⁷³, S. Gonzalez Fernandez¹⁴, R. Gonzalez Lopez⁹¹, C. Gonzalez Renteria¹⁸, R. Gonzalez Suarez¹⁷¹, S. Gonzalez-Sevilla⁵⁴, G.R. Gonzalvo Rodriguez¹⁷³, L. Goossens³⁶, N.A. Gorasia²¹, P.A. Gorbounov¹²⁴, H.A. Gordon²⁹, B. Gorini³⁶, E. Gorini^{68a,68b}, A. Gorišek⁹², A.T. Goshaw⁴⁹, M.I. Gostkin⁸⁰, C.A. Gottardo¹¹⁹, M. Goughri^{35b}, A.G. Goussiou¹⁴⁷, N. Govender^{33c}, C. Goy⁵, I. Grabowska-Bold^{84a}, E.C. Graham⁹¹, J. Gramling¹⁷⁰, E. Gramstad¹³³, S. Grancagnolo¹⁹, M. Grandi¹⁵⁵, V. Gratchev¹³⁷, P.M. Gravila^{27f}, F.G. Gravili^{68a,68b}, C. Gray⁵⁷, H.M. Gray¹⁸, C. Grefe²⁴, K. Gregersen⁹⁷, I.M. Gregor⁴⁶, P. Grenier¹⁵², K. Grevtsov⁴⁶, C. Grieco¹⁴, N.A. Grieser¹²⁸, A.A. Grillo¹⁴⁵, K. Grimm^{31,k}, S. Grinstein^{14,w}, J.-F. Grivaz⁶⁵, S. Groh¹⁰⁰, E. Gross¹⁷⁹, J. Grosse-Knetter⁵³, Z.J. Grout⁹⁵, C. Grud¹⁰⁶, A. Grummer¹¹⁸, J.C. Grundy¹³⁴, L. Guan¹⁰⁶, W. Guan¹⁸⁰, C. Gubbels¹⁷⁴, J. Guenther³⁶, A. Guerguichon⁶⁵, J.G.R. Guerrero Rojas¹⁷³, F. Guescini¹¹⁵, D. Guest¹⁷⁰, R. Gugel¹⁰⁰, A. Guida⁴⁶, T. Guillemain⁵, S. Guindon³⁶, J. Guo^{60c}, W. Guo¹⁰⁶, Y. Guo^{60a}, Z. Guo¹⁰², R. Gupta⁴⁶, S. Gurbuz^{12c}, G. Gustavino¹²⁸, M. Guth⁵², P. Gutierrez¹²⁸, C. Gutsche⁹⁵, C. Guyot¹⁴⁴, C. Gwenlan¹³⁴, C.B. Gwilliam⁹¹, E.S. Haaland¹³³, A. Haas¹²⁵, C. Haber¹⁸, H.K. Hadavand⁸, A. Hadeef^{60a}, M. Haleem¹⁷⁶, J. Haley¹²⁹, J.J. Hall¹⁴⁸, G. Halladjian¹⁰⁷, G.D. Hallewell¹⁰², K. Hamano¹⁷⁵, H. Hamdaoui^{35e}, M. Hamer²⁴, G.N. Hamity⁵⁰, K. Han^{60a,v}, L. Han^{15c}, L. Han^{60a}, S. Han¹⁸, Y.F. Han¹⁶⁶, K. Hanagaki^{82,t}, M. Hance¹⁴⁵, D.M. Handl¹¹⁴, M.D. Hank³⁷, R. Hankache¹³⁵, E. Hansen⁹⁷, J.B. Hansen⁴⁰, J.D. Hansen⁴⁰, M.C. Hansen²⁴, P.H. Hansen⁴⁰, E.C. Hanson¹⁰¹, K. Hara¹⁶⁸, T. Harenberg¹⁸¹, S. Harkusha¹⁰⁸, P.F. Harrison¹⁷⁷, N.M. Hartman¹⁵², N.M. Hartmann¹¹⁴, Y. Hasegawa¹⁴⁹, A. Hasib⁵⁰, S. Hassani¹⁴⁴, S. Haug²⁰, R. Hauser¹⁰⁷, L.B. Havener³⁹, M. Havranek¹⁴¹, C.M. Hawkes²¹, R.J. Hawkings³⁶, S. Hayashida¹¹⁷, D. Hayden¹⁰⁷, C. Hayes¹⁰⁶, R.L. Hayes¹⁷⁴, C.P. Hays¹³⁴, J.M. Hays⁹³, H.S. Hayward⁹¹, S.J. Haywood¹⁴³, F. He^{60a}, Y. He¹⁶⁴, M.P. Heath⁵⁰, V. Hedberg⁹⁷, S. Heer²⁴, A.L. Heggelund¹³³, C. Heidegger⁵², K.K. Heidegger⁵², W.D. Heidorn⁷⁹, J. Heilman³⁴, S. Heim⁴⁶, T. Heim¹⁸, B. Heinemann^{46,aj}, J.G. Heinlein¹³⁶, J.J. Heinrich¹³¹, L. Heinrich³⁶, J. Hejbal¹⁴⁰, L. Helary⁴⁶, A. Held¹²⁵, S. Hellesund¹³³, C.M. Helling¹⁴⁵, S. Hellman^{45a,45b}, C. Helsens³⁶, R.C.W. Henderson⁹⁰, Y. Heng¹⁸⁰, L. Henkelmann³², A.M. Henriques Correia³⁶, H. Herde²⁶, Y. Hernández Jiménez^{33e}, H. Herr¹⁰⁰, M.G. Herrmann¹¹⁴, T. Herrmann⁴⁸, G. Herten⁵², R. Hertenberger¹¹⁴, L. Hervas³⁶, T.C. Herwig¹³⁶, G.G. Hesketh⁹⁵, N.P. Hessey^{167a}, H. Hibi⁸³, S. Higashino⁸², E. Higón-Rodríguez¹⁷³, K. Hildebrand³⁷, J.C. Hill³², K.K. Hill²⁹, K.H. Hiller⁴⁶, S.J. Hillier²¹, M. Hils⁴⁸, I. Hinchliffe¹⁸, F. Hinterkeuser²⁴, M. Hirose¹³², S. Hirose¹⁶⁸, D. Hirschbuehl¹⁸¹, B. Hiti⁹², O. Hladik¹⁴⁰, J. Hobbs¹⁵⁴, N. Hod¹⁷⁹, M.C. Hodgkinson¹⁴⁸, A. Hoecker³⁶, D. Hohn⁵², D. Hohov⁶⁵, T. Holm²⁴, T.R. Holmes³⁷, M. Holzbock¹¹⁵, L.B.A.H. Hommels³², T.M. Hong¹³⁸, J.C. Honig⁵², A. Hönle¹¹⁵, B.H. Hooberman¹⁷², W.H. Hopkins⁶, Y. Horii¹¹⁷, P. Horn⁴⁸, L.A. Horyn³⁷, S. Hou¹⁵⁷, A. Hoummada^{35a}, J. Howarth⁵⁷, J. Hoya⁸⁹, M. Hrabovsky¹³⁰, J. Hrdinka⁷⁷, J. Hrivnac⁶⁵, A. Hrynevich¹⁰⁹, T. Hryn'ova⁵, P.J. Hsu⁶⁴, S.-C. Hsu¹⁴⁷, Q. Hu²⁹, S. Hu^{60c}, Y.F. Hu^{15a,15d,an}, D.P. Huang⁹⁵, X. Huang^{15c}, Y. Huang^{60a}, Y. Huang^{15a}, Z. Hubacek¹⁴¹, F. Hubaut¹⁰², M. Huebner²⁴, F. Huegging²⁴, T.B. Huffman¹³⁴, M. Huhtinen³⁶, R. Hulsken⁵⁸, R.F.H. Hunter³⁴, P. Huo¹⁵⁴, N. Huseynov^{80,ac}, J. Huston¹⁰⁷, J. Huth⁵⁹, R. Hyneman¹⁵², S. Hyrych^{28a}, G. Iacobucci⁵⁴, G. Iakovidis²⁹, I. Ibragimov¹⁵⁰, L. Iconomidou-Fayard⁶⁵, P. Iengo³⁶, R. Ignazzi⁴⁰, O. Igonkina^{120,y,*}, R. Iguchi¹⁶²,

T. Iizawa⁵⁴, Y. Ikegami⁸², M. Ikeno⁸², N. Ilic^{119,166,ab}, F. Iltzsche⁴⁸, H. Imam^{35a}, G. Introzzi^{71a,71b}, M. Iodice^{75a}, K. Iordanidou^{167a}, V. Ippolito^{73a,73b}, M.F. Isacson¹⁷¹, M. Ishino¹⁶², W. Islam¹²⁹, C. Issever^{19,46}, S. Istin¹⁵⁹, J.M. Iturbe Ponce^{63a}, R. Iuppa^{76a,76b}, A. Ivina¹⁷⁹, J.M. Izen⁴³, V. Izzo^{70a}, P. Jacka¹⁴⁰, P. Jackson¹, R.M. Jacobs⁴⁶, B.P. Jaeger¹⁵¹, V. Jain², G. Jäkel¹⁸¹, K.B. Jakobi¹⁰⁰, K. Jakobs⁵², T. Jakoubek¹⁷⁹, J. Jamieson⁵⁷, K.W. Janas^{84a}, R. Jansky⁵⁴, M. Janus⁵³, P.A. Janus^{84a}, G. Jarlskog⁹⁷, A.E. Jaspan⁹¹, N. Javadov^{80,ac}, T. Javůrek³⁶, M. Javurkova¹⁰³, F. Jeanneau¹⁴⁴, L. Jeanty¹³¹, J. Jejelava^{158a}, P. Jenni^{52,c}, N. Jeong⁴⁶, S. Jézéquel⁵, H. Ji¹⁸⁰, J. Jia¹⁵⁴, H. Jiang⁷⁹, Y. Jiang^{60a}, Z. Jiang¹⁵², S. Jiggins⁵², F.A. Jimenez Morales³⁸, J. Jimenez Pena¹¹⁵, S. Jin^{15c}, A. Jinaru^{27b}, O. Jinnouchi¹⁶⁴, H. Jivan^{33e}, P. Johansson¹⁴⁸, K.A. Johns⁷, C.A. Johnson⁶⁶, E. Jones¹⁷⁷, R.W.L. Jones⁹⁰, S.D. Jones¹⁵⁵, T.J. Jones⁹¹, J. Jongmanns^{61a}, J. Jovicevic³⁶, X. Ju¹⁸, J.J. Junggeburth¹¹⁵, A. Juste Rozas^{14,w}, A. Kaczmarzka⁸⁵, M. Kado^{73a,73b}, H. Kagan¹²⁷, M. Kagan¹⁵², A. Kahn³⁹, C. Kahra¹⁰⁰, T. Kaji¹⁷⁸, E. Kajomovitz¹⁵⁹, C.W. Kalderon²⁹, A. Kaluza¹⁰⁰, A. Kamenshchikov¹²³, M. Kaneda¹⁶², N.J. Kang¹⁴⁵, S. Kang⁷⁹, Y. Kano¹¹⁷, J. Kanzaki⁸², L.S. Kaplan¹⁸⁰, D. Kar^{33e}, K. Karava¹³⁴, M.J. Kareem^{167b}, I. Karkanas¹⁶¹, S.N. Karpov⁸⁰, Z.M. Karpova⁸⁰, V. Kartvelishvili⁹⁰, A.N. Karyukhin¹²³, E. Kasimi¹⁶¹, A. Kastanas^{45a,45b}, C. Kato^{60d}, J. Katzy⁴⁶, K. Kawade¹⁴⁹, K. Kawagoe⁸⁸, T. Kawaguchi¹¹⁷, T. Kawamoto¹⁴⁴, G. Kawamura⁵³, E.F. Kay¹⁷⁵, S. Kazakos¹⁴, V.F. Kazanin^{122b,122a}, J.M. Keaveney^{33a}, R. Keeler¹⁷⁵, J.S. Keller³⁴, E. Kellermann⁹⁷, D. Kelsey¹⁵⁵, J.J. Kempster²¹, J. Kendrick²¹, K.E. Kennedy³⁹, O. Kepka¹⁴⁰, S. Kersten¹⁸¹, B.P. Kerševan⁹², S. Ketabchi Haghighat¹⁶⁶, M. Khader¹⁷², F. Khalil-Zada¹³, M. Khandoga¹⁴⁴, A. Khanov¹²⁹, A.G. Kharlamov^{122b,122a}, T. Kharlamova^{122b,122a}, E.E. Khoda¹⁷⁴, A. Khodinov¹⁶⁵, T.J. Khoo⁵⁴, G. Khorauli¹⁷⁶, E. Khramov⁸⁰, J. Khubua^{158b}, S. Kido⁸³, M. Kiehn³⁶, E. Kim¹⁶⁴, Y.K. Kim³⁷, N. Kimura⁹⁵, A. Kirchhoff⁵³, D. Kirchmeier⁴⁸, J. Kirk¹⁴³, A.E. Kiryunin¹¹⁵, T. Kishimoto¹⁶², D.P. Kisliuk¹⁶⁶, V. Kitali⁴⁶, C. Kitsaki¹⁰, O. Kivernyk²⁴, T. Klapdor-Kleingrothaus⁵², M. Klassen^{61a}, C. Klein³⁴, M.H. Klein¹⁰⁶, M. Klein⁹¹, U. Klein⁹¹, K. Kleinknecht¹⁰⁰, P. Klimek¹²¹, A. Klimentov²⁹, T. Klingl²⁴, T. Klioutchnikova³⁶, F.F. Klitzner¹¹⁴, P. Kluit¹²⁰, S. Kluth¹¹⁵, E. Kneringer⁷⁷, E.B.F.G. Knoops¹⁰², A. Knue⁵², D. Kobayashi⁸⁸, M. Kobel⁴⁸, M. Kocian¹⁵², T. Kodama¹⁶², P. Kodys¹⁴², D.M. Koeck¹⁵⁵, P.T. Koenig²⁴, T. Koffas³⁴, N.M. Köhler³⁶, M. Kolb¹⁴⁴, I. Koletsou⁵, T. Komarek¹³⁰, T. Kondo⁸², K. Köneke⁵², A.X.Y. Kong¹, A.C. König¹¹⁹, T. Kono¹²⁶, V. Konstantinides⁹⁵, N. Konstantinidis⁹⁵, B. Konya⁹⁷, R. Kopeliansky⁶⁶, S. Koperny^{84a}, K. Korcyl⁸⁵, K. Kordas¹⁶¹, G. Koren¹⁶⁰, A. Korn⁹⁵, I. Korolkov¹⁴, E.V. Korolkova¹⁴⁸, N. Korotkova¹¹³, O. Kortner¹¹⁵, S. Kortner¹¹⁵, V.V. Kostyukhin^{148,165}, A. Kotskechagia⁶⁵, A. Kotwal⁴⁹, A. Koulouris¹⁰, A. Kourkouveli-Charalampidi^{71a,71b}, C. Kourkouvelis⁹, E. Kourlitis⁶, V. Kouskoura²⁹, R. Kowalewski¹⁷⁵, W. Kozanecki¹⁰¹, A.S. Kozhin¹²³, V.A. Kramarenko¹¹³, G. Kramberger⁹², D. Krasnopevtsev^{60a}, M.W. Krasny¹³⁵, A. Krasznahorkay³⁶, D. Krauss¹¹⁵, J.A. Kremer¹⁰⁰, J. Kretzschmar⁹¹, P. Krieger¹⁶⁶, F. Krieter¹¹⁴, A. Krishnan^{61b}, M. Krivos¹⁴², K. Krizka¹⁸, K. Kroeninger⁴⁷, H. Kroha¹¹⁵, J. Kroll¹⁴⁰, J. Kroll¹³⁶, K.S. Krowpman¹⁰⁷, U. Kruchonak⁸⁰, H. Krüger²⁴, N. Krumnack⁷⁹, M.C. Kruse⁴⁹, J.A. Krzysiaik⁸⁵, A. Kubota¹⁶⁴, O. Kuchinskaia¹⁶⁵, S. Kuday^{4b}, J.T. Kuechler⁴⁶, S. Kuehn³⁶, T. Kuhl⁴⁶, V. Kukhtin⁸⁰, Y. Kulchitsky^{108,ae}, S. Kuleshov^{146b}, Y.P. Kulinich¹⁷², M. Kuna⁵⁸, A. Kupco¹⁴⁰, T. Kupfer⁴⁷, O. Kuprash⁵², H. Kurashige⁸³, L.L. Kurchaninov^{167a}, Y.A. Kurochkin¹⁰⁸, A. Kurova¹¹², M.G. Kurth^{15a,15d}, E.S. Kuwertz³⁶, M. Kuze¹⁶⁴, A.K. Kvam¹⁴⁷, J. Kvita¹³⁰, T. Kwan¹⁰⁴, F. La Ruffa^{41b,41a}, C. Lacasta¹⁷³, F. Lacava^{73a,73b}, D.P.J. Lack¹⁰¹, H. Lacker¹⁹, D. Lacour¹³⁵, E. Ladygin⁸⁰, R. Lafaye⁵, B. Laforge¹³⁵, T. Lagouri^{146c}, S. Lai⁵³, I.K. Lakomic^{84a}, J.E. Lambert¹²⁸, S. Lammers⁶⁶, W. Lampl⁷, C. Lampoudis¹⁶¹, E. Lançon²⁹, U. Landgraf⁵², M.P.J. Landon⁹³, M.C. Lanfermann⁵⁴, V.S. Lang⁵², J.C. Lange⁵³, R.J. Langenberg¹⁰³, A.J. Lankford¹⁷⁰, F. Lanni²⁹, K. Lantzsche²⁴, A. Lanza^{71a}, A. Lapertosa^{55b,55a}, J.F. Laporte¹⁴⁴, T. Lari^{69a}, F. Lasagni Manghi^{23b,23a}, M. Lassnig³⁶, T.S. Lau^{63a}, A. Laudrain¹⁰⁰, A. Laurier³⁴, M. Lavorgna^{70a,70b}, S.D. Lawlor⁹⁴, M. Lazzaroni^{69a,69b}, B. Le¹⁰¹, E. Le Guirriec¹⁰², A. Lebedev⁷⁹, M. LeBlanc⁷, T. LeCompte⁶, F. Ledroit-Guillon⁵⁸, A.C.A. Lee⁹⁵, C.A. Lee²⁹, G.R. Lee¹⁷, L. Lee⁵⁹, S.C. Lee¹⁵⁷, S. Lee⁷⁹, B. Lefebvre^{167a}, H.P. Lefebvre⁹⁴, M. Lefebvre¹⁷⁵, C. Leggett¹⁸, K. Lehmann¹⁵¹, N. Lehmann²⁰, G. Lehmann Miotto³⁶, W.A. Leight⁴⁶, A. Leisos^{161,u}, M.A.L. Leite^{81d}, C.E. Leitgeb¹¹⁴, R. Leitner¹⁴², D. Lellouch^{179,*}, K.J.C. Leney⁴², T. Lenz²⁴, S. Leone^{72a}, C. Leonidopoulos⁵⁰, A. Leopold¹³⁵, C. Leroy¹¹⁰, R. Les¹⁰⁷, C.G. Lester³², M. Levchenko¹³⁷, J. Levêque⁵, D. Levin¹⁰⁶, L.J. Levinson¹⁷⁹, D.J. Lewis²¹, B. Li^{15b}, B. Li¹⁰⁶, C.-Q. Li^{60a}, F. Li^{60c}, H. Li^{60a}, H. Li^{60b}, J. Li^{60c}, K. Li¹⁴⁷, L. Li^{60c}, M. Li^{15a,15d}, Q. Li^{15a,15d}, Q.Y. Li^{60a}, S. Li^{60d,60c}, X. Li⁴⁶, Y. Li⁴⁶, Z. Li^{60b}, Z. Li¹³⁴, Z. Li¹⁰⁴, Z. Liang^{15a}, M. Liberatore⁴⁶, B. Liberti^{74a}, A. Liblong¹⁶⁶, K. Lie^{63c}, S. Lim²⁹, C.Y. Lin³², K. Lin¹⁰⁷, R.A. Linck⁶⁶, R.E. Lindley⁷, J.H. Lindon²¹, A. Linss⁴⁶, A.L. Lioni⁵⁴, E. Lipeles¹³⁶,

A. Lipniacka¹⁷, T.M. Liss^{172,ak}, A. Lister¹⁷⁴, J.D. Little⁸, B. Liu⁷⁹, B.L. Liu¹⁵¹, H.B. Liu²⁹, J.B. Liu^{60a}, J.K.K. Liu³⁷, K. Liu^{60d}, M. Liu^{60a}, M.Y. Liu^{60a}, P. Liu^{15a}, X. Liu^{60a}, Y. Liu⁴⁶, Y. Liu^{15a,15d}, Y.L. Liu¹⁰⁶, Y.W. Liu^{60a}, M. Livan^{71a,71b}, A. Lleres⁵⁸, J. Llorente Merino¹⁵¹, S.L. Lloyd⁹³, C.Y. Lo^{63b}, E.M. Lobodzinska⁴⁶, P. Loch⁷, S. Loffredo^{74a,74b}, T. Lohse¹⁹, K. Lohwasser¹⁴⁸, M. Lokajicek¹⁴⁰, J.D. Long¹⁷², R.E. Long⁹⁰, I. Longarini^{73a,73b}, L. Longo³⁶, K.A. Looper¹²⁷, I. Lopez Paz¹⁰¹, A. Lopez Solis¹⁴⁸, J. Lorenz¹¹⁴, N. Lorenzo Martinez⁵, A.M. Lory¹¹⁴, P.J. Lösel¹¹⁴, A. Lösle⁵², X. Lou^{45a,45b}, X. Lou^{15a}, A. Lounis⁶⁵, J. Love⁶, P.A. Love⁹⁰, J.J. Lozano Bahilo¹⁷³, M. Lu^{60a}, Y.J. Lu⁶⁴, H.J. Lubatti¹⁴⁷, C. Luci^{73a,73b}, F.L. Lucio Alves^{15c}, A. Lucotte⁵⁸, F. Luehring⁶⁶, I. Luise¹³⁵, L. Luminari^{73a}, B. Lund-Jensen¹⁵³, M.S. Lutz¹⁶⁰, D. Lynn²⁹, H. Lyons⁹¹, R. Lysak¹⁴⁰, E. Lytken⁹⁷, F. Lyu^{15a}, V. Lyubushkin⁸⁰, T. Lyubushkina⁸⁰, H. Ma²⁹, L.L. Ma^{60b}, Y. Ma⁹⁵, D.M. Mac Donell¹⁷⁵, G. Maccarrone⁵¹, A. Macchiolo¹¹⁵, C.M. Macdonald¹⁴⁸, J.C. MacDonald¹⁴⁸, J. Machado Miguens¹³⁶, D. Madaffari¹⁷³, R. Madar³⁸, W.F. Mader⁴⁸, M. Madugoda Ralalage Don¹²⁹, N. Madysa⁴⁸, J. Maeda⁸³, T. Maeno²⁹, M. Maerker⁴⁸, V. Magerl⁵², N. Magini⁷⁹, J. Magro^{67a,67c,q}, D.J. Mahon³⁹, C. Maidantchik^{81b}, T. Maier¹¹⁴, A. Maio^{139a,139b,139d}, K. Maj^{84a}, O. Majersky^{28a}, S. Majewski¹³¹, Y. Makida⁸², N. Makovec⁶⁵, B. Malaescu¹³⁵, Pa. Malecki⁸⁵, V.P. Maleev¹³⁷, F. Malek⁵⁸, D. Malito^{41b,41a}, U. Mallik⁷⁸, D. Malon⁶, C. Malone³², S. Maltezos¹⁰, S. Malyukov⁸⁰, J. Mamuzic¹⁷³, G. Mancini^{70a,70b}, I. Mandić⁹², L. Manhaes de Andrade Filho^{81a}, I.M. Maniatis¹⁶¹, J. Manjarres Ramos⁴⁸, K.H. Mankinen⁹⁷, A. Mann¹¹⁴, A. Manousos⁷⁷, B. Mansoulie¹⁴⁴, I. Mantos¹⁶¹, S. Manzoni¹²⁰, A. Marantis¹⁶¹, G. Marceca³⁰, L. Marchese¹³⁴, G. Marchiori¹³⁵, M. Marcisovsky¹⁴⁰, L. Marcoccia^{74a,74b}, C. Marcon⁹⁷, M. Marjanovic¹²⁸, Z. Marshall¹⁸, M.U.F. Martensson¹⁷¹, S. Marti-Garcia¹⁷³, C.B. Martin¹²⁷, T.A. Martin¹⁷⁷, V.J. Martin⁵⁰, B. Martin dit Latour¹⁷, L. Martinelli^{75a,75b}, M. Martinez^{14,w}, P. Martinez Agullo¹⁷³, V.I. Martinez Outschoorn¹⁰³, S. Martin-Haugh¹⁴³, V.S. Martoiu^{27b}, A.C. Martyniuk⁹⁵, A. Marzin³⁶, S.R. Maschek¹¹⁵, L. Masetti¹⁰⁰, T. Mashimo¹⁶², R. Mashinistov¹¹¹, J. Masik¹⁰¹, A.L. Maslennikov^{122b,122a}, L. Massa^{23b,23a}, P. Massarotti^{70a,70b}, P. Mastrandrea^{72a,72b}, A. Mastroberardino^{41b,41a}, T. Masubuchi¹⁶², D. Matakias²⁹, A. Matic¹¹⁴, N. Matsuzawa¹⁶², P. Mättig²⁴, J. Maurer^{27b}, B. Maček⁹², D.A. Maximov^{122b,122a}, R. Mazini¹⁵⁷, I. Maznas¹⁶¹, S.M. Mazza¹⁴⁵, J.P. Mc Gowan¹⁰⁴, S.P. Mc Kee¹⁰⁶, T.G. McCarthy¹¹⁵, W.P. McCormack¹⁸, E.F. McDonald¹⁰⁵, A.E. Mcdougall¹²⁰, J.A. Mcfayden¹⁸, G. Mchedlidze^{158b}, M.A. McKay⁴², K.D. McLean¹⁷⁵, S.J. McMahon¹⁴³, P.C. McNamara¹⁰⁵, C.J. McNicol¹⁷⁷, R.A. McPherson^{175,ab}, J.E. Mdhluli^{33e}, Z.A. Meadows¹⁰³, S. Meehan³⁶, T. Megy³⁸, S. Mehlhase¹¹⁴, A. Mehta⁹¹, B. Meirose⁴³, D. Melini¹⁵⁹, B.R. Mellado Garcia^{33e}, J.D. Mellenthin⁵³, M. Melo^{28a}, F. Meloni⁴⁶, A. Melzer²⁴, E.D. Mendes Gouveia^{139a,139e}, A.M. Mendes Jacques Da Costa²¹, L. Meng³⁶, X.T. Meng¹⁰⁶, S. Menke¹¹⁵, E. Meoni^{41b,41a}, S. Mergelmeyer¹⁹, S.A.M. Merkt¹³⁸, C. Merlassino¹³⁴, P. Mermod⁵⁴, L. Merola^{70a,70b}, C. Meroni^{69a}, G. Merz¹⁰⁶, O. Meshkov^{113,111}, J.K.R. Meshreki¹⁵⁰, J. Metcalfe⁶, A.S. Mete⁶, C. Meyer⁶⁶, J-P. Meyer¹⁴⁴, M. Michetti¹⁹, R.P. Middleton¹⁴³, L. Mijović⁵⁰, G. Mikenberg¹⁷⁹, M. Mikestikova¹⁴⁰, M. Mikuž⁹², H. Mildner¹⁴⁸, A. Milic¹⁶⁶, C.D. Milke⁴², D.W. Miller³⁷, A. Milov¹⁷⁹, D.A. Milstead^{45a,45b}, R.A. Mina¹⁵², A.A. Minaenko¹²³, I.A. Minashvili^{158b}, A.I. Mincer¹²⁵, B. Mindur^{84a}, M. Mineev⁸⁰, Y. Minegishi¹⁶², Y. Mino⁸⁶, L.M. Mir¹⁴, M. Mironova¹³⁴, A. Mirto^{68a,68b}, K.P. Mistry¹³⁶, T. Mitani¹⁷⁸, J. Mitrevski¹¹⁴, V.A. Mitsou¹⁷³, M. Mittal^{60c}, O. Miu¹⁶⁶, A. Miucci²⁰, P.S. Miyagawa⁹³, A. Mizukami⁸², J.U. Mjörnmark⁹⁷, T. Mkrtchyan^{61a}, M. Mlynarikova¹⁴², T. Moa^{45a,45b}, S. Mobius⁵³, K. Mochizuki¹¹⁰, P. Mogg¹¹⁴, S. Mohapatra³⁹, R. Moles-Valls²⁴, K. Mönig⁴⁶, E. Monnier¹⁰², A. Montalbano¹⁵¹, J. Montejo Berlingen³⁶, M. Montella⁹⁵, F. Monticelli⁸⁹, S. Monzani^{69a}, K. Moor⁵³, N. Morange⁶⁵, A.L. Moreira De Carvalho^{139a}, D. Moreno^{22a}, M. Moreno Llácer¹⁷³, C. Moreno Martinez¹⁴, P. Morettini^{55b}, M. Morgenstern¹⁵⁹, S. Morgenstern⁴⁸, D. Mori¹⁵¹, M. Morii⁵⁹, M. Morinaga¹⁷⁸, V. Morisbak¹³³, A.K. Morley³⁶, G. Mornacchi³⁶, A.P. Morris⁹⁵, L. Morvaj¹⁵⁴, P. Moschovakos³⁶, B. Moser¹²⁰, M. Mosidze^{158b}, T. Moskalets¹⁴⁴, J. Moss^{31,m}, E.J.W. Moyse¹⁰³, S. Muanza¹⁰², J. Mueller¹³⁸, R.S.P. Mueller¹¹⁴, D. Muenstermann⁹⁰, G.A. Mullier⁹⁷, D.P. Mungo^{69a,69b}, J.L. Munoz Martinez¹⁴, F.J. Munoz Sanchez¹⁰¹, P. Murin^{28b}, W.J. Murray^{177,143}, A. Murrone^{69a,69b}, J.M. Muse¹²⁸, M. Muškinja¹⁸, C. Mwewa^{33a}, A.G. Myagkov^{123,ag}, A.A. Myers¹³⁸, G. Myers⁶⁶, J. Myers¹³¹, M. Myska¹⁴¹, B.P. Nachman¹⁸, O. Nackenhorst⁴⁷, A. Nag Nag⁴⁸, K. Nagai¹³⁴, K. Nagano⁸², Y. Nagasaka⁶², J.L. Nagle²⁹, E. Nagy¹⁰², A.M. Nairz³⁶, Y. Nakahama¹¹⁷, K. Nakamura⁸², T. Nakamura¹⁶², H. Nanjo¹³², F. Napolitano^{61a}, R.F. Naranjo Garcia⁴⁶, R. Narayan⁴², I. Naryshkin¹³⁷, M. Naseri³⁴, T. Naumann⁴⁶, G. Navarro^{22a}, P.Y. Nechaeva¹¹¹, F. Nechansky⁴⁶, T.J. Neep²¹, A. Negri^{71a,71b}, M. Negrini^{23b},

C. Nellist¹¹⁹, C. Nelson¹⁰⁴, M.E. Nelson^{45a,45b}, S. Nemecek¹⁴⁰, M. Nessi^{36,e}, M.S. Neubauer¹⁷², F. Neuhaus¹⁰⁰, M. Neumann¹⁸¹, R. Newhouse¹⁷⁴, P.R. Newman²¹, C.W. Ng¹³⁸, Y.S. Ng¹⁹, Y.W.Y. Ng¹⁷⁰, B. Ngair^{35e}, H.D.N. Nguyen¹⁰², T. Nguyen Manh¹¹⁰, E. Nibigira³⁸, R.B. Nickerson¹³⁴, R. Nicolaidou¹⁴⁴, D.S. Nielsen⁴⁰, J. Nielsen¹⁴⁵, M. Niemeyer⁵³, N. Nikiforou¹¹, V. Nikolaenko^{123,ag}, I. Nikolic-Audit¹³⁵, K. Nikolopoulos²¹, P. Nilsson²⁹, H.R. Nindhito⁵⁴, A. Nisati^{73a}, N. Nishu^{60c}, R. Nisius¹¹⁵, I. Nitsche⁴⁷, T. Nitta¹⁷⁸, T. Nobe¹⁶², D.L. Noel³², Y. Noguchi⁸⁶, I. Nomidis¹³⁵, M.A. Nomura²⁹, M. Nordberg³⁶, J. Novak⁹², T. Novak⁹², O. Novgorodova⁴⁸, R. Novotny¹⁴¹, L. Nozka¹³⁰, K. Ntekas¹⁷⁰, E. Nurse⁹⁵, F.G. Oakham^{34,al}, H. Oberlack¹¹⁵, J. Ocariz¹³⁵, A. Ochi⁸³, I. Ochoa³⁹, J.P. Ochoa-Ricoux^{146a}, K. O'Connor²⁶, S. Oda⁸⁸, S. Odaka⁸², S. Oerdek⁵³, A. Ogrodnik^{84a}, A. Oh¹⁰¹, C.C. Ohm¹⁵³, H. Oide¹⁶⁴, M.L. Ojeda¹⁶⁶, H. Okawa¹⁶⁸, Y. Okazaki⁸⁶, M.W. O'Keefe⁹¹, Y. Okumura¹⁶², A. Olariu^{27b}, L.F. Oleiro Seabra^{139a}, S.A. Olivares Pino^{146a}, D. Oliveira Damazio²⁹, J.L. Oliver¹, M.J.R. Olsson¹⁷⁰, A. Olszewski⁸⁵, J. Olszowska⁸⁵, Ö.O. Öncel²⁴, D.C. O'Neil¹⁵¹, A.P. O'Neill¹³⁴, A. Onofre^{139a,139e}, P.U.E. Onyisi¹¹, H. Oppen¹³³, R.G. Oreamuno Madriz¹²¹, M.J. Oreglia³⁷, G.E. Orellana⁸⁹, D. Orestano^{75a,75b}, N. Orlando¹⁴, R.S. Orr¹⁶⁶, V. O'Shea⁵⁷, R. Ospanov^{60a}, G. Otero y Garzon³⁰, H. Otono⁸⁸, P.S. Ott^{61a}, G.J. Ottino¹⁸, M. Ouchrif^{35d}, J. Ouellette²⁹, F. Ould-Saada¹³³, A. Ouraou¹⁴⁴, Q. Ouyang^{15a}, M. Owen⁵⁷, R.E. Owen¹⁴³, V.E. Ozcan^{12c}, N. Ozturk⁸, J. Pacalt¹³⁰, H.A. Pacey³², K. Pachal⁴⁹, A. Pacheco Pages¹⁴, C. Padilla Aranda¹⁴, S. Pagan Griso¹⁸, G. Palacino⁶⁶, S. Palazzo⁵⁰, S. Palestini³⁶, M. Palka^{84b}, P. Palni^{84a}, C.E. Pandini⁵⁴, J.G. Panduro Vazquez⁹⁴, P. Pani⁴⁶, G. Panizzo^{67a,67c}, L. Paolozzi⁵⁴, C. Papadatos¹¹⁰, K. Papageorgiou^{9,g}, S. Parajuli⁴², A. Paramonov⁶, C. Paraskevopoulos¹⁰, D. Paredes Hernandez^{63b}, S.R. Paredes Saenz¹³⁴, B. Parida¹⁷⁹, T.H. Park¹⁶⁶, A.J. Parker³¹, M.A. Parker³², F. Parodi^{55b,55a}, E.W. Parrish¹²¹, J.A. Parsons³⁹, U. Parzefall⁵², L. Pascual Dominguez¹³⁵, V.R. Pascuzzi¹⁸, J.M.P. Pasner¹⁴⁵, F. Pasquali¹²⁰, E. Pasqualucci^{73a}, S. Passaggio^{55b}, F. Pastore⁹⁴, P. Pasuwan^{45a,45b}, S. Pataria¹⁰⁰, J.R. Pater¹⁰¹, A. Pathak^{180,i}, J. Patton⁹¹, T. Pauly³⁶, J. Pearkes¹⁵², B. Pearson¹¹⁵, M. Pedersen¹³³, L. Pedraza Diaz¹¹⁹, R. Pedro^{139a}, T. Peiffer⁵³, S.V. Peleganchuk^{122b,122a}, O. Penc¹⁴⁰, H. Peng^{60a}, B.S. Peralva^{81a}, M.M. Perego⁶⁵, A.P. Pereira Peixoto^{139a}, L. Pereira Sanchez^{45a,45b}, D.V. Perepelitsa²⁹, E. Perez Codina^{167a}, F. Peri¹⁹, L. Perini^{69a,69b}, H. Pernegger³⁶, S. Perrella³⁶, A. Perrevoort¹²⁰, K. Peters⁴⁶, R.F.Y. Peters¹⁰¹, B.A. Petersen³⁶, T.C. Petersen⁴⁰, E. Petit¹⁰², V. Petousis¹⁴¹, A. Petridis¹, C. Petridou¹⁶¹, P. Petroff⁶⁵, F. Petrucci^{75a,75b}, M. Pettee¹⁸², N.E. Pettersson¹⁰³, K. Petukhova¹⁴², A. Peyaud¹⁴⁴, R. Pezoa^{146d}, L. Pezzotti^{71a,71b}, T. Pham¹⁰⁵, P.W. Phillips¹⁴³, M.W. Phipps¹⁷², G. Piacquadio¹⁵⁴, E. Pianori¹⁸, A. Picazio¹⁰³, R.H. Pickles¹⁰¹, R. Piegaia³⁰, D. Pietreanu^{27b}, J.E. Pilcher³⁷, A.D. Pilkington¹⁰¹, M. Pinamonti^{67a,67c}, J.L. Pinfold³, C. Pitman Donaldson⁹⁵, M. Pitt¹⁶⁰, L. Pizzimento^{74a,74b}, A. Pizzini¹²⁰, M.-A. Pleier²⁹, V. Plesanovs⁵², V. Pleskot¹⁴², E. Plotnikova⁸⁰, P. Podberezko^{122b,122a}, R. Poettgen⁹⁷, R. Poggi⁵⁴, L. Poggioli¹³⁵, I. Pogrebnnyak¹⁰⁷, D. Pohl²⁴, I. Pokharel⁵³, G. Polesello^{71a}, A. Poley^{151,167a}, A. Policicchio^{73a,73b}, R. Polifka¹⁴², A. Polini^{23b}, C.S. Pollard⁴⁶, V. Polychronakos²⁹, D. Ponomarenko¹¹², L. Pontecorvo³⁶, S. Popa^{27a}, G.A. Popeneciu^{27d}, L. Portales⁵, D.M. Portillo Quintero⁵⁸, S. Pospisil¹⁴¹, K. Potamianos⁴⁶, I.N. Potrap⁸⁰, C.J. Potter³², H. Potti¹¹, T. Poulsen⁹⁷, J. Poveda¹⁷³, T.D. Powell¹⁴⁸, G. Pownall⁴⁶, M.E. Pozo Astigarraga³⁶, A. Prades Ibanez¹⁷³, P. Pralavorio¹⁰², S. Prell⁷⁹, D. Price¹⁰¹, M. Primavera^{68a}, M.L. Proffitt¹⁴⁷, N. Proklova¹¹², K. Prokofiev^{63c}, F. Prokoshin⁸⁰, S. Protopopescu²⁹, J. Proudfoot⁶, M. Przybycien^{84a}, D. Pudzha¹³⁷, A. Puri¹⁷², P. Puzo⁶⁵, D. Pyatiizbyantseva¹¹², J. Qian¹⁰⁶, Y. Qin¹⁰¹, A. Quadt⁵³, M. Queitsch-Maitland³⁶, M. Racko^{28a}, F. Ragusa^{69a,69b}, G. Rahal⁹⁸, J.A. Raine⁵⁴, S. Rajagopalan²⁹, A. Ramirez Morales⁹³, K. Ran^{15a,15d}, D.M. Rauch⁴⁶, F. Rauscher¹¹⁴, S. Rave¹⁰⁰, B. Ravina⁵⁷, I. Ravinovitch¹⁷⁹, J.H. Rawling¹⁰¹, M. Raymond³⁶, A.L. Read¹³³, N.P. Readioff¹⁴⁸, M. Reale^{68a,68b}, D.M. Rebuzzi^{71a,71b}, G. Redlinger²⁹, K. Reeves⁴³, J. Reichert¹³⁶, D. Reikher¹⁶⁰, A. Reiss¹⁰⁰, A. Rej¹⁵⁰, C. Rembser³⁶, A. Renardi⁴⁶, M. Renda^{27b}, M.B. Rendel¹¹⁵, A.G. Rennie⁵⁷, S. Resconi^{69a}, E.D. Resseguie¹⁸, S. Rettie⁹⁵, B. Reynolds¹²⁷, E. Reynolds²¹, O.L. Rezanova^{122b,122a}, P. Reznicek¹⁴², E. Ricci^{76a,76b}, R. Richter¹¹⁵, S. Richter⁴⁶, E. Richter-Was^{84b}, M. Ridet¹³⁵, P. Rieck¹¹⁵, O. Rifki⁴⁶, M. Rijssenbeek¹⁵⁴, A. Rimoldi^{71a,71b}, M. Rimoldi⁴⁶, L. Rinaldi^{23b}, T.T. Rinn¹⁷², G. Ripellino¹⁵³, I. Riu¹⁴, P. Rivadeneira⁴⁶, J.C. Rivera Vergara¹⁷⁵, F. Rizatdinova¹²⁹, E. Rizvi⁹³, C. Rizzi³⁶, S.H. Robertson^{104,ab}, M. Robin⁴⁶, D. Robinson³², C.M. Robles Gajardo^{146d}, M. Robles Manzano¹⁰⁰, A. Robson⁵⁷, A. Rocchi^{74a,74b}, E. Rocco¹⁰⁰, C. Roda^{72a,72b}, S. Rodriguez Bosca¹⁷³, A.M. Rodríguez Vera^{167b}, S. Roe³⁶, J. Roggel¹⁸¹, O. Røhne¹³³, R. Röhrig¹¹⁵, R.A. Rojas^{146d}, B. Roland⁵², C.P.A. Roland⁶⁶, J. Roloff²⁹, A. Romaniouk¹¹², M. Romano^{23b,23a}, N. Rompotis⁹¹, M. Ronzani¹²⁵,

L. Roos¹³⁵, S. Rosati^{73a}, G. Rosin¹⁰³, B.J. Rosser¹³⁶, E. Rossi⁴⁶, E. Rossi^{75a,75b}, E. Rossi^{70a,70b}, L.P. Rossi^{55b}, L. Rossini⁴⁶, R. Rosten¹⁴, M. Rotaru^{27b}, B. Rottler⁵², D. Rousseau⁶⁵, G. Rovelli^{71a,71b}, A. Roy¹¹, D. Roy^{33e}, A. Rozanov¹⁰², Y. Rozen¹⁵⁹, X. Ruan^{33e}, T.A. Ruggeri¹, F. Rühr⁵², A. Ruiz-Martinez¹⁷³, A. Rummler³⁶, Z. Rurikova⁵², N.A. Rusakovich⁸⁰, H.L. Russell¹⁰⁴, L. Rustige^{38,47}, J.P. Rutherford⁷, E.M. Rüttinger¹⁴⁸, M. Rybar¹⁴², G. Rybkin⁶⁵, E.B. Rye¹³³, A. Ryzhov¹²³, J.A. Sabater Iglesias⁴⁶, P. Sabatini⁵³, L. Sabetta^{73a,73b}, S. Sacerdoti⁶⁵, H.F.-W. Sadrozinski¹⁴⁵, R. Sadykov⁸⁰, F. Safai Tehrani^{73a}, B. Safarzadeh Samani¹⁵⁵, M. Safdari¹⁵², P. Saha¹²¹, S. Saha¹⁰⁴, M. Sahinsoy¹¹⁵, A. Sahu¹⁸¹, M. Saimpert³⁶, M. Saito¹⁶², T. Saito¹⁶², H. Sakamoto¹⁶², D. Salamani⁵⁴, G. Salamanna^{75a,75b}, A. Salnikov¹⁵², J. Salt¹⁷³, A. Salvador Salas¹⁴, D. Salvatore^{41b,41a}, F. Salvatore¹⁵⁵, A. Salvucci^{63a,63b,63c}, A. Salzburger³⁶, J. Samarati³⁶, D. Sammel⁵², D. Sampsonidis¹⁶¹, D. Sampsonidou¹⁶¹, J. Sánchez¹⁷³, A. Sanchez Pineda^{67a,36,67c}, H. Sandaker¹³³, C.O. Sander⁴⁶, I.G. Sanderswood⁹⁰, M. Sandhoff¹⁸¹, C. Sandoval^{22b}, D.P.C. Sankey¹⁴³, M. Sannino^{55b,55a}, Y. Sano¹¹⁷, A. Sansoni⁵¹, C. Santoni³⁸, H. Santos^{139a,139b}, S.N. Santpur¹⁸, A. Santra¹⁷³, K.A. Saoucha¹⁴⁸, A. Sapronov⁸⁰, J.G. Saraiva^{139a,139d}, O. Sasaki⁸², K. Sato¹⁶⁸, F. Sauerburger⁵², E. Sauvan⁵, P. Savard^{166,al}, R. Sawada¹⁶², C. Sawyer¹⁴³, L. Sawyer^{96,af}, I. Sayago Galvan¹⁷³, C. Sbarra^{23b}, A. Sbrizzi^{67a,67c}, T. Scanlon⁹⁵, J. Schaarschmidt¹⁴⁷, P. Schacht¹¹⁵, D. Schaefer³⁷, L. Schaefer¹³⁶, S. Schaepe³⁶, U. Schäfer¹⁰⁰, A.C. Schaffer⁶⁵, D. Schaile¹¹⁴, R.D. Schamberger¹⁵⁴, E. Schanet¹¹⁴, C. Scharf¹⁹, N. Scharmberg¹⁰¹, V.A. Schegelsky¹³⁷, D. Scheirich¹⁴², F. Schenck¹⁹, M. Schernau¹⁷⁰, C. Schiavi^{55b,55a}, L.K. Schildgen²⁴, Z.M. Schillaci²⁶, E.J. Schioppa^{68a,68b}, M. Schioppa^{41b,41a}, K.E. Schleicher⁵², S. Schlenker³⁶, K.R. Schmidt-Sommerfeld¹¹⁵, K. Schmieden³⁶, C. Schmitt¹⁰⁰, S. Schmitt⁴⁶, L. Schoeffel¹⁴⁴, A. Schoening^{61b}, P.G. Scholer⁵², E. Schopf¹³⁴, M. Schott¹⁰⁰, J.F.P. Schouwenberg¹¹⁹, J. Schovancova³⁶, S. Schramm⁵⁴, F. Schroeder¹⁸¹, A. Schulte¹⁰⁰, H.-C. Schultz-Coulon^{61a}, M. Schumacher⁵², B.A. Schumm¹⁴⁵, Ph. Schune¹⁴⁴, A. Schwartzman¹⁵², T.A. Schwarz¹⁰⁶, Ph. Schwemling¹⁴⁴, R. Schwienhorst¹⁰⁷, A. Sciandra¹⁴⁵, G. Sciolla²⁶, M. Scornajenghi^{41b,41a}, F. Scuri^{72a}, F. Scutti¹⁰⁵, L.M. Scyboz¹¹⁵, C.D. Sebastiani⁹¹, P. Seema¹⁹, S.C. Seidel¹¹⁸, A. Seiden¹⁴⁵, B.D. Seidlitz²⁹, T. Seiss³⁷, C. Seitz⁴⁶, J.M. Seixas^{81b}, G. Sekhniaidze^{70a}, S.J. Sekula⁴², N. Semprini-Cesari^{23b,23a}, S. Sen⁴⁹, C. Serfon²⁹, L. Serin⁶⁵, L. Serkin^{67a,67b}, M. Sessa^{60a}, H. Severini¹²⁸, S. Sevova¹⁵², F. Sforza^{55b,55a}, A. Sfyrly⁵⁴, E. Shabalina⁵³, J.D. Shahinian¹⁴⁵, N.W. Shaikh^{45a,45b}, D. Shaked Renous¹⁷⁹, L.Y. Shan^{15a}, M. Shapiro¹⁸, A. Sharma¹³⁴, A.S. Sharma¹, P.B. Shatalov¹²⁴, K. Shaw¹⁵⁵, S.M. Shaw¹⁰¹, M. Shehade¹⁷⁹, Y. Shen¹²⁸, A.D. Sherman²⁵, P. Sherwood⁹⁵, L. Shi⁹⁵, C.O. Shimmin¹⁸², Y. Shimogama¹⁷⁸, M. Shimojima¹¹⁶, I.P.J. Shipsey¹³⁴, S. Shirabe¹⁶⁴, M. Shiyakova^{80,z}, J. Shlomi¹⁷⁹, A. Shmeleva¹¹¹, M.J. Shochet³⁷, J. Shojaii¹⁰⁵, D.R. Shope¹⁵³, S. Shrestha¹²⁷, E.M. Shrif^{33e}, M.J. Shroff¹⁷⁵, E. Shulga¹⁷⁹, P. Sicho¹⁴⁰, A.M. Sickles¹⁷², E. Sideras Haddad^{33e}, O. Sidiropoulou³⁶, A. Sidoti^{23b,23a}, F. Siegert⁴⁸, Dj. Sijacki¹⁶, M.Jr. Silva¹⁸⁰, M.V. Silva Oliveira³⁶, S.B. Silverstein^{45a}, S. Simion⁶⁵, R. Simoniello¹⁰⁰, C.J. Simpson-allsoy²¹, S. Simsek^{12b}, P. Sinervo¹⁶⁶, V. Sinetckii¹¹³, S. Singh¹⁵¹, M. Sioli^{23b,23a}, I. Siral¹³¹, S.Yu. Sivoklov¹¹³, J. Sjölin^{45a,45b}, A. Skaf⁵³, E. Skorda⁹⁷, P. Skubic¹²⁸, M. Slawinska⁸⁵, K. Sliwa¹⁶⁹, R. Slovak¹⁴², V. Smakhtin¹⁷⁹, B.H. Smart¹⁴³, J. Smiesko^{28b}, N. Smirnov¹¹², S.Yu. Smirnov¹¹², Y. Smirnov¹¹², L.N. Smirnova^{113,r}, O. Smirnova⁹⁷, E.A. Smith³⁷, H.A. Smith¹³⁴, M. Smizanska⁹⁰, K. Smolek¹⁴¹, A. Smykiewicz⁸⁵, A.A. Snesev¹¹¹, H.L. Snoek¹²⁰, I.M. Snyder¹³¹, S. Snyder²⁹, R. Sobie^{175,ab}, A. Soffer¹⁶⁰, A. Søgaard⁵⁰, F. Sohns⁵³, C.A. Solans Sanchez³⁶, E.Yu. Soldatov¹¹², U. Soldevila¹⁷³, A.A. Solodkov¹²³, A. Soloshenko⁸⁰, O.V. Solovyanov¹²³, V. Solovye¹³⁷, P. Sommer¹⁴⁸, H. Son¹⁶⁹, A. Sonay¹⁴, W. Song¹⁴³, W.Y. Song^{167b}, A. Sopczak¹⁴¹, A.L. Sopio⁹⁵, F. Sopkova^{28b}, S. Sottocornola^{71a,71b}, R. Soualah^{67a,67c}, A.M. Soukharev^{122b,122a}, D. South⁴⁶, S. Spagnolo^{68a,68b}, M. Spalla¹¹⁵, M. Spangenberg¹⁷⁷, F. Spanò⁹⁴, D. Sperlich⁵², T.M. Spieker^{61a}, G. Spigo³⁶, M. Spina¹⁵⁵, D.P. Spiteri⁵⁷, M. Spousta¹⁴², A. Stabile^{69a,69b}, B.L. Stamas¹²¹, R. Stamen^{61a}, M. Stamenkovic¹²⁰, A. Stampeki²¹, E. Stanecka⁸⁵, B. Stanislaus¹³⁴, M.M. Stanitzki⁴⁶, M. Stankaityte¹³⁴, B. Stapf¹²⁰, E.A. Starchenko¹²³, G.H. Stark¹⁴⁵, J. Stark⁵⁸, P. Staroba¹⁴⁰, P. Starovoitov^{61a}, S. Stärz¹⁰⁴, R. Staszewski⁸⁵, G. Stavropoulos⁴⁴, M. Stegler⁴⁶, P. Steinberg²⁹, A.L. Steinhebel¹³¹, B. Stelzer^{151,167a}, H.J. Stelzer¹³⁸, O. Stelzer-Chilton^{167a}, H. Stenzel⁵⁶, T.J. Stevenson¹⁵⁵, G.A. Stewart³⁶, M.C. Stockton³⁶, G. Stoica^{27b}, M. Stolarski^{139a}, S. Stonjek¹¹⁵, A. Straessner⁴⁸, J. Strandberg¹⁵³, S. Strandberg^{45a,45b}, M. Strauss¹²⁸, T. Strebl¹⁰², P. Strizenec^{28b}, R. Ströhmer¹⁷⁶, D.M. Strom¹³¹, R. Stroynowski⁴², A. Strubig⁵⁰, S.A. Stucci²⁹, B. Stugu¹⁷, J. Stupak¹²⁸, N.A. Styles⁴⁶, D. Su¹⁵², W. Su^{60c,147}, X. Su^{60a}, V.V. Sulin¹¹¹, M.J. Sullivan⁹¹, D.M.S. Sultan⁵⁴, S. Sultansoy^{4c}, T. Sumida⁸⁶, S. Sun¹⁰⁶, X. Sun¹⁰¹, C.J.E. Suster¹⁵⁶,

M.R. Sutton¹⁵⁵, S. Suzuki⁸², M. Svatos¹⁴⁰, M. Swiatlowski^{167a}, S.P. Swift², T. Swirski¹⁷⁶,
A. Sydorenko¹⁰⁰, I. Sykora^{28a}, M. Sykora¹⁴², T. Sykora¹⁴², D. Ta¹⁰⁰, K. Tackmann^{46,x}, J. Taenzer¹⁶⁰,
A. Taffard¹⁷⁰, R. Tafirout^{167a}, E. Tagiev¹²³, R. Takashima⁸⁷, K. Takeda⁸³, T. Takeshita¹⁴⁹, E.P. Takeva⁵⁰,
Y. Takubo⁸², M. Talby¹⁰², A.A. Talyshv^{122b,122a}, K.C. Tam^{63b}, N.M. Tamir¹⁶⁰, J. Tanaka¹⁶², R. Tanaka⁶⁵,
S. Tapia Araya¹⁷², S. Tapprogge¹⁰⁰, A. Tarek Abouelfadl Mohamed¹⁰⁷, S. Tarem¹⁵⁹, K. Tariq^{60b},
G. Tarna^{27b,d}, G.F. Tartarelli^{69a}, P. Tas¹⁴², M. Tasevsky¹⁴⁰, E. Tassi^{41b,41a}, A. Tavares Delgado^{139a},
Y. Tayalati^{35e}, A.J. Taylor⁵⁰, G.N. Taylor¹⁰⁵, W. Taylor^{167b}, H. Teagle⁹¹, A.S. Tee⁹⁰,
R. Teixeira De Lima¹⁵², P. Teixeira-Dias⁹⁴, H. Ten Kate³⁶, J.J. Teoh¹²⁰, K. Terashi¹⁶², J. Terron⁹⁹,
S. Terzo¹⁴, M. Testa⁵¹, R.J. Teuscher^{166,ab}, S.J. Thais¹⁸², N. Themistokleous⁵⁰, T. Theveneaux-Pelzer⁴⁶,
F. Thiele⁴⁰, D.W. Thomas⁹⁴, J.O. Thomas⁴², J.P. Thomas²¹, E.A. Thompson⁴⁶, P.D. Thompson²¹,
E. Thomson¹³⁶, E.J. Thorpe⁹³, R.E. Ticse Torres⁵³, V.O. Tikhomirov^{111,ah}, Yu.A. Tikhonov^{122b,122a},
S. Timoshenko¹¹², P. Tipton¹⁸², S. Tisserant¹⁰², K. Todome^{23b,23a}, S. Todorova-Nova¹⁴², S. Todt⁴⁸,
J. Tojo⁸⁸, S. Tokár^{28a}, K. Tokushuku⁸², E. Tolley¹²⁷, R. Tombs³², K.G. Tomiwa^{33e}, M. Tomoto¹¹⁷,
L. Tompkins¹⁵², P. Tornambe¹⁰³, E. Torrence¹³¹, H. Torres⁴⁸, E. Torró Pastor¹⁷³, C. Toscirì¹³⁴,
J. Toth^{102,aa}, D.R. Tovey¹⁴⁸, A. Traet¹⁷, C.J. Treado¹²⁵, T. Trefzger¹⁷⁶, F. Tresoldi¹⁵⁵, A. Tricoli²⁹,
I.M. Trigger^{167a}, S. Trincas-Duvoid¹³⁵, D.A. Trischuk¹⁷⁴, W. Trischuk¹⁶⁶, B. Trocmé⁵⁸, A. Trofymov⁶⁵,
C. Troncon^{69a}, F. Trovato¹⁵⁵, L. Truong^{33c}, M. Trzebinski⁸⁵, A. Trzupek⁸⁵, F. Tsai⁴⁶, J.C.-L. Tseng¹³⁴,
P.V. Tsiarashka^{108,ae}, A. Tsigotis^{161,u}, V. Tsiskaridze¹⁵⁴, E.G. Tskhadadze^{158a}, M. Tsopoulou¹⁶¹,
I.I. Tsukerman¹²⁴, V. Tsulaia¹⁸, S. Tsuno⁸², D. Tsybychev¹⁵⁴, Y. Tu^{63b}, A. Tudorache^{27b}, V. Tudorache^{27b},
T.T. Tulbure^{27a}, A.N. Tuna⁵⁹, S. Turchikhin⁸⁰, D. Turgeman¹⁷⁹, I. Turk Cakir^{4b,s}, R.J. Turner²¹,
R. Turra^{69a}, P.M. Tuts³⁹, S. Tzamarias¹⁶¹, E. Tzovara¹⁰⁰, K. Uchida¹⁶², F. Ukegawa¹⁶⁸, G. Unal³⁶,
M. Unal¹¹, A. Undrus²⁹, G. Unel¹⁷⁰, F.C. Ungaro¹⁰⁵, Y. Unno⁸², K. Uno¹⁶², J. Urban^{28b}, P. Urquijo¹⁰⁵,
G. Usai⁸, Z. Uysal^{12d}, V. Vacek¹⁴¹, B. Vachon¹⁰⁴, K.O.H. Vadla¹³³, T. Vafeiadis³⁶, A. Vaidya⁹⁵,
C. Valderanis¹¹⁴, E. Valdes Santurio^{45a,45b}, M. Valente⁵⁴, S. Valentinetti^{23b,23a}, A. Valero¹⁷³, L. Valéry⁴⁶,
R.A. Vallance²¹, A. Vallier³⁶, J.A. Valls Ferrer¹⁷³, T.R. Van Daalen¹⁴, P. Van Gemmeren⁶, S. Van Stroud⁹⁵,
I. Van Vulpen¹²⁰, M. Vanadia^{74a,74b}, W. Vandelli³⁶, M. Vandenbroucke¹⁴⁴, E.R. Vandewall¹²⁹,
A. Vaniachine¹⁶⁵, D. Vannicola^{73a,73b}, R. Vari^{73a}, E.W. Varnes⁷, C. Varni^{55b,55a}, T. Varol¹⁵⁷,
D. Varouchas⁶⁵, K.E. Varvell¹⁵⁶, M.E. Vasile^{27b}, G.A. Vasquez¹⁷⁵, F. Vazeille³⁸, D. Vazquez Furelos¹⁴,
T. Vazquez Schroeder³⁶, J. Veatch⁵³, V. Vecchio¹⁰¹, M.J. Veen¹²⁰, L.M. Veloce¹⁶⁶, F. Veloso^{139a,139c},
S. Veneziano^{73a}, A. Ventura^{68a,68b}, A. Verbytskyi¹¹⁵, V. Vercesi^{71a}, M. Verducci^{72a,72b},
C.M. Vergel Infante⁷⁹, C. Vergis²⁴, W. Verkerke¹²⁰, A.T. Vermeulen¹²⁰, J.C. Vermeulen¹²⁰, C. Vernieri¹⁵²,
P.J. Verschuuren⁹⁴, M.C. Vetterli^{151,al}, N. Viaux Maira^{146d}, T. Vickey¹⁴⁸, O.E. Vickey Boeriu¹⁴⁸,
G.H.A. Viehhauser¹³⁴, L. Vignani^{61b}, M. Villa^{23b,23a}, M. Villaplana Perez³, E.M. Villhauer⁵⁰, E. Vilucchi⁵¹,
M.G. Vinciter³⁴, G.S. Virdee²¹, A. Vishwakarma⁵⁰, C. Vittori^{23b,23a}, I. Vivarelli¹⁵⁵, M. Vogel¹⁸¹,
P. Vokac¹⁴¹, S.E. von Buddenbrock^{33e}, E. Von Toerne²⁴, V. Vorobel¹⁴², K. Vorobev¹¹², M. Vos¹⁷³,
J.H. Vosseveld⁹¹, M. Vozak¹⁰¹, N. Vranjes¹⁶, M. Vranjes Milosavljevic¹⁶, V. Vrba¹⁴¹, M. Vreeswijk¹²⁰,
N.K. Vu¹⁰², R. Vuillermet³⁶, I. Vukotic³⁷, S. Wada¹⁶⁸, P. Wagner²⁴, W. Wagner¹⁸¹, J. Wagner-Kuhr¹¹⁴,
S. Wahdan¹⁸¹, H. Wahlberg⁸⁹, R. Wakasa¹⁶⁸, V.M. Walbrecht¹¹⁵, J. Walder¹⁴³, R. Walker¹¹⁴,
S.D. Walker⁹⁴, W. Walkowiak¹⁵⁰, V. Wallangen^{45a,45b}, A.M. Wang⁵⁹, A.Z. Wang¹⁸⁰, C. Wang^{60a},
C. Wang^{60c}, F. Wang¹⁸⁰, H. Wang¹⁸, H. Wang³, J. Wang^{63a}, P. Wang⁴², Q. Wang¹²⁸, R.-J. Wang¹⁰⁰,
R. Wang^{60a}, R. Wang⁶, S.M. Wang¹⁵⁷, W.T. Wang^{60a}, W. Wang^{15c}, W.X. Wang^{60a}, Y. Wang^{60a},
Z. Wang¹⁰⁶, C. Wanotayaroj⁴⁶, A. Warburton¹⁰⁴, C.P. Ward³², R.J. Ward²¹, N. Warrack⁵⁷, A.T. Watson²¹,
M.F. Watson²¹, G. Watts¹⁴⁷, B.M. Waugh⁹⁵, A.F. Webb¹¹, C. Weber²⁹, M.S. Weber²⁰, S.A. Weber³⁴,
S.M. Weber^{61a}, A.R. Weidberg¹³⁴, J. Weingarten⁴⁷, M. Weirich¹⁰⁰, C. Weiser⁵², P.S. Wells³⁶,
T. Wenaus²⁹, B. Wendland⁴⁷, T. Wengler³⁶, S. Wenig³⁶, N. Wermes²⁴, M. Wessels^{61a}, T.D. Weston²⁰,
K. Whalen¹³¹, A.M. Wharton⁹⁰, A.S. White¹⁰⁶, A. White⁸, M.J. White¹, D. Whiteson¹⁷⁰,
B.W. Whitmore⁹⁰, W. Wiedenmann¹⁸⁰, C. Wiel⁴⁸, M. Wielers¹⁴³, N. Wieseotte¹⁰⁰, C. Wigglesworth⁴⁰,
L.A.M. Wiik-Fuchs⁵², H.G. Wilkens³⁶, L.J. Wilkins⁹⁴, H.H. Williams¹³⁶, S. Williams³², S. Willocq¹⁰³,
P.J. Windischhofer¹³⁴, I. Wingerter-Seez⁵, E. Winkels¹⁵⁵, F. Winklmeier¹³¹, B.T. Winter⁵²,
M. Wittgen¹⁵², M. Wobisch⁹⁶, A. Wolf¹⁰⁰, R. Wölker¹³⁴, J. Wollrath⁵², M.W. Wolter⁸⁵,
H. Wolters^{139a,139c}, V.W.S. Wong¹⁷⁴, N.L. Woods¹⁴⁵, S.D. Worm⁴⁶, B.K. Wosiek⁸⁵, K.W. Woźniak⁸⁵,
K. Wraight⁵⁷, S.L. Wu¹⁸⁰, X. Wu⁵⁴, Y. Wu^{60a}, J. Wuerzinger¹³⁴, T.R. Wyatt¹⁰¹, B.M. Wynne⁵⁰, S. Xella⁴⁰,
L. Xia¹⁷⁷, J. Xiang^{63c}, X. Xiao¹⁰⁶, X. Xie^{60a}, I. Xiotidis¹⁵⁵, D. Xu^{15a}, H. Xu^{60a}, H. Xu^{60a}, L. Xu²⁹,

T. Xu¹⁴⁴, W. Xu¹⁰⁶, Z. Xu^{60b}, Z. Xu¹⁵², B. Yabsley¹⁵⁶, S. Yacoob^{33a}, D.P. Yallup⁹⁵, N. Yamaguchi⁸⁸, Y. Yamaguchi¹⁶⁴, A. Yamamoto⁸², M. Yamatani¹⁶², T. Yamazaki¹⁶², Y. Yamazaki⁸³, J. Yan^{60c}, Z. Yan²⁵, H.J. Yang^{60c,60d}, H.T. Yang¹⁸, S. Yang^{60a}, T. Yang^{63c}, X. Yang^{60b,58}, Y. Yang¹⁶², Z. Yang^{60a}, W.-M. Yao¹⁸, Y.C. Yap⁴⁶, E. Yatsenko^{60c}, H. Ye^{15c}, J. Ye⁴², S. Ye²⁹, I. Yeletsikh⁸⁰, M.R. Yexley⁹⁰, E. Yigitbasi²⁵, P. Yin³⁹, K. Yorita¹⁷⁸, K. Yoshihara⁷⁹, C.J.S. Young³⁶, C. Young¹⁵², J. Yu⁷⁹, R. Yuan^{60b,h}, X. Yue^{61a}, M. Zaazoua^{35e}, B. Zabinski⁸⁵, G. Zacharis¹⁰, E. Zaffaroni⁵⁴, J. Zahreddine¹³⁵, A.M. Zaitsev^{123,ag}, T. Zakareishvili^{158b}, N. Zakharchuk³⁴, S. Zambito³⁶, D. Zanzi³⁶, S.V. ZeiBner⁴⁷, C. Zeitnitz¹⁸¹, G. Zemaityte¹³⁴, J.C. Zeng¹⁷², O. Zenin¹²³, T. Ženiš^{28a}, D. Zerwas⁶⁵, M. Zgubič¹³⁴, B. Zhang^{15c}, D.F. Zhang^{15b}, G. Zhang^{15b}, J. Zhang⁶, Kaili. Zhang^{15a}, L. Zhang^{15c}, L. Zhang^{60a}, M. Zhang¹⁷², R. Zhang¹⁸⁰, S. Zhang¹⁰⁶, X. Zhang^{60c}, X. Zhang^{60b}, Y. Zhang^{15a,15d}, Z. Zhang^{63a}, Z. Zhang⁶⁵, P. Zhao⁴⁹, Z. Zhao^{60a}, A. Zhemchugov⁸⁰, Z. Zheng¹⁰⁶, D. Zhong¹⁷², B. Zhou¹⁰⁶, C. Zhou¹⁸⁰, H. Zhou⁷, M.S. Zhou^{15a,15d}, M. Zhou¹⁵⁴, N. Zhou^{60c}, Y. Zhou⁷, C.G. Zhu^{60b}, C. Zhu^{15a,15d}, H.L. Zhu^{60a}, H. Zhu^{15a}, J. Zhu¹⁰⁶, Y. Zhu^{60a}, X. Zhuang^{15a}, K. Zhukov¹¹¹, V. Zhulanov^{122b,122a}, D. Zieminska⁶⁶, N.I. Zimine⁸⁰, S. Zimmermann⁵², Z. Zinonos¹¹⁵, M. Ziolkowski¹⁵⁰, L. Živković¹⁶, G. Zobernig¹⁸⁰, A. Zoccoli^{23b,23a}, K. Zoch⁵³, T.G. Zorbas¹⁴⁸, R. Zou³⁷, L. Zwalinski³⁶

¹ Department of Physics, University of Adelaide, Adelaide; Australia

² Physics Department, SUNY Albany, Albany NY; United States of America

³ Department of Physics, University of Alberta, Edmonton AB; Canada

⁴ (a) Department of Physics, Ankara University, Ankara; (b) Istanbul Aydin University, Application and Research Center for Advanced Studies, Istanbul; (c) Division of Physics, TOBB University of Economics and Technology, Ankara; Turkey

⁵ LAPP, Université Grenoble Alpes, Université Savoie Mont Blanc, CNRS/IN2P3, Annecy; France

⁶ High Energy Physics Division, Argonne National Laboratory, Argonne IL; United States of America

⁷ Department of Physics, University of Arizona, Tucson AZ; United States of America

⁸ Department of Physics, University of Texas at Arlington, Arlington TX; United States of America

⁹ Physics Department, National and Kapodistrian University of Athens, Athens; Greece

¹⁰ Physics Department, National Technical University of Athens, Zografou; Greece

¹¹ Department of Physics, University of Texas at Austin, Austin TX; United States of America

¹² (a) Bahcesehir University, Faculty of Engineering and Natural Sciences, Istanbul; (b) Istanbul Bilgi University, Faculty of Engineering and Natural Sciences, Istanbul; (c) Department of Physics, Bogazici University, Istanbul; (d) Department of Physics Engineering, Gaziantep University, Gaziantep; Turkey

¹³ Institute of Physics, Azerbaijan Academy of Sciences, Baku; Azerbaijan

¹⁴ Institut de Física d'Altes Energies (IFAE), Barcelona Institute of Science and Technology, Barcelona; Spain

¹⁵ (a) Institute of High Energy Physics, Chinese Academy of Sciences, Beijing; (b) Physics Department, Tsinghua University, Beijing; (c) Department of Physics, Nanjing University, Nanjing;

(d) University of Chinese Academy of Science (UCAS), Beijing; China

¹⁶ Institute of Physics, University of Belgrade, Belgrade; Serbia

¹⁷ Department for Physics and Technology, University of Bergen, Bergen; Norway

¹⁸ Physics Division, Lawrence Berkeley National Laboratory and University of California, Berkeley CA; United States of America

¹⁹ Institut für Physik, Humboldt Universität zu Berlin, Berlin; Germany

²⁰ Albert Einstein Center for Fundamental Physics and Laboratory for High Energy Physics, University of Bern, Bern; Switzerland

²¹ School of Physics and Astronomy, University of Birmingham, Birmingham; United Kingdom

²² (a) Facultad de Ciencias y Centro de Investigaciones, Universidad Antonio Nariño, Bogotá; (b) Departamento de Física, Universidad Nacional de Colombia, Bogotá; Colombia

²³ (a) INFN Bologna and Università di Bologna, Dipartimento di Fisica; (b) INFN Sezione di Bologna; Italy

²⁴ Physikalisches Institut, Universität Bonn, Bonn; Germany

²⁵ Department of Physics, Boston University, Boston MA; United States of America

²⁶ Department of Physics, Brandeis University, Waltham MA; United States of America

²⁷ (a) Transilvania University of Brasov, Brasov; (b) Horia Hulubei National Institute of Physics and Nuclear Engineering, Bucharest; (c) Department of Physics, Alexandru Ioan Cuza University of Iasi, Iasi; (d) National Institute for Research and Development of Isotopic and Molecular Technologies, Physics Department, Cluj-Napoca; (e) University Politehnica Bucharest, Bucharest; (f) West University in Timisoara, Timisoara; Romania

²⁸ (a) Faculty of Mathematics, Physics and Informatics, Comenius University, Bratislava; (b) Department of Subnuclear Physics, Institute of Experimental Physics of the Slovak Academy of Sciences, Kosice; Slovak Republic

²⁹ Physics Department, Brookhaven National Laboratory, Upton NY; United States of America

³⁰ Departamento de Física, Universidad de Buenos Aires, Buenos Aires; Argentina

³¹ California State University, CA; United States of America

³² Cavendish Laboratory, University of Cambridge, Cambridge; United Kingdom

³³ (a) Department of Physics, University of Cape Town, Cape Town; (b) iThemba Labs, Western Cape; (c) Department of Mechanical Engineering Science, University of Johannesburg, Johannesburg; (d) University of South Africa, Department of Physics, Pretoria; (e) School of Physics, University of the Witwatersrand, Johannesburg; South Africa

³⁴ Department of Physics, Carleton University, Ottawa ON; Canada

³⁵ (a) Faculté des Sciences Ain Chock, Réseau Universitaire de Physique des Hautes Energies – Université Hassan II, Casablanca; (b) Faculté des Sciences, Université Ibn-Tofail, Kénitra;

(c) Faculté des Sciences Semlalia, Université Cadi Ayyad, LPHEA, Marrakech; (d) Faculté des Sciences, Université Mohamed Premier and LPTPM, Oujda; (e) Faculté des sciences, Université Mohammed V, Rabat; Morocco

³⁶ CERN, Geneva; Switzerland

³⁷ Enrico Fermi Institute, University of Chicago, Chicago IL; United States of America

³⁸ LPC, Université Clermont Auvergne, CNRS/IN2P3, Clermont-Ferrand; France

³⁹ Nevis Laboratory, Columbia University, Irvington NY; United States of America

⁴⁰ Niels Bohr Institute, University of Copenhagen, Copenhagen; Denmark

⁴¹ (a) Dipartimento di Fisica, Università della Calabria, Rende; (b) INFN Gruppo Collegato di Cosenza, Laboratori Nazionali di Frascati; Italy

⁴² Physics Department, Southern Methodist University, Dallas TX; United States of America

⁴³ Physics Department, University of Texas at Dallas, Richardson TX; United States of America

⁴⁴ National Centre for Scientific Research "Demokritos", Agia Paraskevi; Greece

⁴⁵ (a) Department of Physics, Stockholm University; (b) Oskar Klein Centre, Stockholm; Sweden

⁴⁶ Deutsches Elektronen-Synchrotron DESY, Hamburg and Zeuthen; Germany

⁴⁷ Lehrstuhl für Experimentelle Physik IV, Technische Universität Dortmund, Dortmund; Germany

⁴⁸ Institut für Kern- und Teilchenphysik, Technische Universität Dresden, Dresden; Germany

- ⁴⁹ Department of Physics, Duke University, Durham NC; United States of America
- ⁵⁰ SUPA – School of Physics and Astronomy, University of Edinburgh, Edinburgh; United Kingdom
- ⁵¹ INFN e Laboratori Nazionali di Frascati, Frascati; Italy
- ⁵² Physikalisches Institut, Albert-Ludwigs-Universität Freiburg, Freiburg; Germany
- ⁵³ II. Physikalisches Institut, Georg-August-Universität Göttingen, Göttingen; Germany
- ⁵⁴ Département de Physique Nucléaire et Corpusculaire, Université de Genève, Genève; Switzerland
- ⁵⁵ ^(a) Dipartimento di Fisica, Università di Genova, Genova; ^(b) INFN Sezione di Genova; Italy
- ⁵⁶ II. Physikalisches Institut, Justus-Liebig-Universität Giessen, Giessen; Germany
- ⁵⁷ SUPA – School of Physics and Astronomy, University of Glasgow, Glasgow; United Kingdom
- ⁵⁸ LPSC, Université Grenoble Alpes, CNRS/IN2P3, Grenoble INP, Grenoble; France
- ⁵⁹ Laboratory for Particle Physics and Cosmology, Harvard University, Cambridge MA; United States of America
- ⁶⁰ ^(a) Department of Modern Physics and State Key Laboratory of Particle Detection and Electronics, University of Science and Technology of China, Hefei; ^(b) Institute of Frontier and Interdisciplinary Science and Key Laboratory of Particle Physics and Particle Irradiation (MOE), Shandong University, Qingdao; ^(c) School of Physics and Astronomy, Shanghai Jiao Tong University, KLPPAC-MoE, SKLPPC, Shanghai; ^(d) Tsung-Dao Lee Institute, Shanghai; China
- ⁶¹ ^(a) Kirchhoff-Institut für Physik, Ruprecht-Karls-Universität Heidelberg, Heidelberg; ^(b) Physikalisches Institut, Ruprecht-Karls-Universität Heidelberg, Heidelberg; Germany
- ⁶² Faculty of Applied Information Science, Hiroshima Institute of Technology, Hiroshima; Japan
- ⁶³ ^(a) Department of Physics, Chinese University of Hong Kong, Shatin, N.T., Hong Kong; ^(b) Department of Physics, University of Hong Kong, Hong Kong; ^(c) Department of Physics and Institute for Advanced Study, Hong Kong University of Science and Technology, Clear Water Bay, Kowloon, Hong Kong; China
- ⁶⁴ Department of Physics, National Tsing Hua University, Hsinchu; Taiwan
- ⁶⁵ IJCLab, Université Paris-Saclay, CNRS/IN2P3, 91405, Orsay; France
- ⁶⁶ Department of Physics, Indiana University, Bloomington IN; United States of America
- ⁶⁷ ^(a) INFN Gruppo Collegato di Udine, Sezione di Trieste, Udine; ^(b) ICTP, Trieste; ^(c) Dipartimento Politecnico di Ingegneria e Architettura, Università di Udine, Udine; Italy
- ⁶⁸ ^(a) INFN Sezione di Lecce; ^(b) Dipartimento di Matematica e Fisica, Università del Salento, Lecce; Italy
- ⁶⁹ ^(a) INFN Sezione di Milano; ^(b) Dipartimento di Fisica, Università di Milano, Milano; Italy
- ⁷⁰ ^(a) INFN Sezione di Napoli; ^(b) Dipartimento di Fisica, Università di Napoli, Napoli; Italy
- ⁷¹ ^(a) INFN Sezione di Pavia; ^(b) Dipartimento di Fisica, Università di Pavia, Pavia; Italy
- ⁷² ^(a) INFN Sezione di Pisa; ^(b) Dipartimento di Fisica E. Fermi, Università di Pisa, Pisa; Italy
- ⁷³ ^(a) INFN Sezione di Roma; ^(b) Dipartimento di Fisica, Sapienza Università di Roma, Roma; Italy
- ⁷⁴ ^(a) INFN Sezione di Roma Tor Vergata; ^(b) Dipartimento di Fisica, Università di Roma Tor Vergata, Roma; Italy
- ⁷⁵ ^(a) INFN Sezione di Roma Tre; ^(b) Dipartimento di Matematica e Fisica, Università Roma Tre, Roma; Italy
- ⁷⁶ ^(a) INFN-TIFPA; ^(b) Università degli Studi di Trento, Trento; Italy
- ⁷⁷ Institut für Astro- und Teilchenphysik, Leopold-Franzens-Universität, Innsbruck; Austria
- ⁷⁸ University of Iowa, Iowa City IA; United States of America
- ⁷⁹ Department of Physics and Astronomy, Iowa State University, Ames IA; United States of America
- ⁸⁰ Joint Institute for Nuclear Research, Dubna; Russia
- ⁸¹ ^(a) Departamento de Engenharia Elétrica, Universidade Federal de Juiz de Fora (UFJF), Juiz de Fora; ^(b) Universidade Federal do Rio De Janeiro COPPE/EE/IF, Rio de Janeiro; ^(c) Universidade Federal de São João del Rei (UFJSJ), São João del Rei; ^(d) Instituto de Física, Universidade de São Paulo, São Paulo; Brazil
- ⁸² KEK, High Energy Accelerator Research Organization, Tsukuba; Japan
- ⁸³ Graduate School of Science, Kobe University, Kobe; Japan
- ⁸⁴ ^(a) AGH University of Science and Technology, Faculty of Physics and Applied Computer Science, Krakow; ^(b) Marian Smoluchowski Institute of Physics, Jagiellonian University, Krakow; Poland
- ⁸⁵ Institute of Nuclear Physics Polish Academy of Sciences, Krakow; Poland
- ⁸⁶ Faculty of Science, Kyoto University, Kyoto; Japan
- ⁸⁷ Kyoto University of Education, Kyoto; Japan
- ⁸⁸ Research Center for Advanced Particle Physics and Department of Physics, Kyushu University, Fukuoka; Japan
- ⁸⁹ Instituto de Física La Plata, Universidad Nacional de La Plata and CONICET, La Plata; Argentina
- ⁹⁰ Physics Department, Lancaster University, Lancaster; United Kingdom
- ⁹¹ Oliver Lodge Laboratory, University of Liverpool, Liverpool; United Kingdom
- ⁹² Department of Experimental Particle Physics, Jožef Stefan Institute and Department of Physics, University of Ljubljana, Ljubljana; Slovenia
- ⁹³ School of Physics and Astronomy, Queen Mary University of London, London; United Kingdom
- ⁹⁴ Department of Physics, Royal Holloway University of London, Egham; United Kingdom
- ⁹⁵ Department of Physics and Astronomy, University College London, London; United Kingdom
- ⁹⁶ Louisiana Tech University, Ruston LA; United States of America
- ⁹⁷ Fysiska institutionen, Lunds universitet, Lund; Sweden
- ⁹⁸ Centre de Calcul de l'Institut National de Physique Nucléaire et de Physique des Particules (IN2P3), Villeurbanne; France
- ⁹⁹ Departamento de Física Teórica C-15 and CIAFF, Universidad Autónoma de Madrid, Madrid; Spain
- ¹⁰⁰ Institut für Physik, Universität Mainz, Mainz; Germany
- ¹⁰¹ School of Physics and Astronomy, University of Manchester, Manchester; United Kingdom
- ¹⁰² CPPM, Aix-Marseille Université, CNRS/IN2P3, Marseille; France
- ¹⁰³ Department of Physics, University of Massachusetts, Amherst MA; United States of America
- ¹⁰⁴ Department of Physics, McGill University, Montreal QC; Canada
- ¹⁰⁵ School of Physics, University of Melbourne, Victoria; Australia
- ¹⁰⁶ Department of Physics, University of Michigan, Ann Arbor MI; United States of America
- ¹⁰⁷ Department of Physics and Astronomy, Michigan State University, East Lansing MI; United States of America
- ¹⁰⁸ B.I. Stepanov Institute of Physics, National Academy of Sciences of Belarus, Minsk; Belarus
- ¹⁰⁹ Research Institute for Nuclear Problems of Byelorussian State University, Minsk; Belarus
- ¹¹⁰ Group of Particle Physics, University of Montreal, Montreal QC; Canada
- ¹¹¹ P.N. Lebedev Physical Institute of the Russian Academy of Sciences, Moscow; Russia
- ¹¹² National Research Nuclear University MEPhI, Moscow; Russia
- ¹¹³ D.V. Skobeltsyn Institute of Nuclear Physics, M.V. Lomonosov Moscow State University, Moscow; Russia
- ¹¹⁴ Fakultät für Physik, Ludwig-Maximilians-Universität München, München; Germany
- ¹¹⁵ Max-Planck-Institut für Physik (Werner-Heisenberg-Institut), München; Germany
- ¹¹⁶ Nagasaki Institute of Applied Science, Nagasaki; Japan
- ¹¹⁷ Graduate School of Science and Kobayashi-Maskawa Institute, Nagoya University, Nagoya; Japan
- ¹¹⁸ Department of Physics and Astronomy, University of New Mexico, Albuquerque NM; United States of America
- ¹¹⁹ Institute for Mathematics, Astrophysics and Particle Physics, Radboud University Nijmegen/Nikhef, Nijmegen; Netherlands
- ¹²⁰ Nikhef National Institute for Subatomic Physics and University of Amsterdam, Amsterdam; Netherlands
- ¹²¹ Department of Physics, Northern Illinois University, DeKalb IL; United States of America
- ¹²² ^(a) Budker Institute of Nuclear Physics and NSU, SB RAS, Novosibirsk; ^(b) Novosibirsk State University Novosibirsk; Russia
- ¹²³ Institute for High Energy Physics of the National Research Centre Kurchatov Institute, Protvino; Russia

- ¹²⁴ Institute for Theoretical and Experimental Physics named by A.I. Alikhanov of National Research Centre “Kurchatov Institute”, Moscow; Russia
- ¹²⁵ Department of Physics, New York University, New York NY; United States of America
- ¹²⁶ Ochanomizu University, Otsuka, Bunkyo-ku, Tokyo; Japan
- ¹²⁷ Ohio State University, Columbus OH; United States of America
- ¹²⁸ Homer L. Dodge Department of Physics and Astronomy, University of Oklahoma, Norman OK; United States of America
- ¹²⁹ Department of Physics, Oklahoma State University, Stillwater OK; United States of America
- ¹³⁰ Palacký University, RPTM, Joint Laboratory of Optics, Olomouc; Czech Republic
- ¹³¹ Institute for Fundamental Science, University of Oregon, Eugene, OR; United States of America
- ¹³² Graduate School of Science, Osaka University, Osaka; Japan
- ¹³³ Department of Physics, University of Oslo, Oslo; Norway
- ¹³⁴ Department of Physics, Oxford University, Oxford; United Kingdom
- ¹³⁵ LPNHE, Sorbonne Université, Université de Paris, CNRS/IN2P3, Paris; France
- ¹³⁶ Department of Physics, University of Pennsylvania, Philadelphia PA; United States of America
- ¹³⁷ Konstantinov Nuclear Physics Institute of National Research Centre “Kurchatov Institute”, PNPI, St. Petersburg; Russia
- ¹³⁸ Department of Physics and Astronomy, University of Pittsburgh, Pittsburgh PA; United States of America
- ¹³⁹ ^(a) Laboratório de Instrumentação e Física Experimental de Partículas – LIP, Lisboa; ^(b) Departamento de Física, Faculdade de Ciências, Universidade de Lisboa, Lisboa; ^(c) Departamento de Física, Universidade de Coimbra, Coimbra; ^(d) Centro de Física Nuclear da Universidade de Lisboa, Lisboa; ^(e) Departamento de Física, Universidade do Minho, Braga; ^(f) Departamento de Física Teórica y del Cosmos, Universidad de Granada, Granada (Spain); ^(g) Dep Física and CEFITEC de Faculdade de Ciências e Tecnologia, Universidade Nova de Lisboa, Caparica;
- ^(h) Instituto Superior Técnico, Universidade de Lisboa, Lisboa; Portugal
- ¹⁴⁰ Institute of Physics of the Czech Academy of Sciences, Prague; Czech Republic
- ¹⁴¹ Czech Technical University in Prague, Prague; Czech Republic
- ¹⁴² Charles University, Faculty of Mathematics and Physics, Prague; Czech Republic
- ¹⁴³ Particle Physics Department, Rutherford Appleton Laboratory, Didcot; United Kingdom
- ¹⁴⁴ IRFU, CEA, Université Paris-Saclay, Gif-sur-Yvette; France
- ¹⁴⁵ Santa Cruz Institute for Particle Physics, University of California Santa Cruz, Santa Cruz CA; United States of America
- ¹⁴⁶ ^(a) Departamento de Física, Pontificia Universidad Católica de Chile, Santiago; ^(b) Universidad Andres Bello, Department of Physics, Santiago; ^(c) Instituto de Alta Investigación, Universidad de Tarapacá; ^(d) Departamento de Física, Universidad Técnica Federico Santa María, Valparaíso; Chile
- ¹⁴⁷ Department of Physics, University of Washington, Seattle WA; United States of America
- ¹⁴⁸ Department of Physics and Astronomy, University of Sheffield, Sheffield; United Kingdom
- ¹⁴⁹ Department of Physics, Shinshu University, Nagano; Japan
- ¹⁵⁰ Department Physik, Universität Siegen, Siegen; Germany
- ¹⁵¹ Department of Physics, Simon Fraser University, Burnaby BC; Canada
- ¹⁵² SLAC National Accelerator Laboratory, Stanford CA; United States of America
- ¹⁵³ Physics Department, Royal Institute of Technology, Stockholm; Sweden
- ¹⁵⁴ Departments of Physics and Astronomy, Stony Brook University, Stony Brook NY; United States of America
- ¹⁵⁵ Department of Physics and Astronomy, University of Sussex, Brighton; United Kingdom
- ¹⁵⁶ School of Physics, University of Sydney, Sydney; Australia
- ¹⁵⁷ Institute of Physics, Academia Sinica, Taipei; Taiwan
- ¹⁵⁸ ^(a) E. Andronikashvili Institute of Physics, Iv. Javakishvili Tbilisi State University, Tbilisi; ^(b) High Energy Physics Institute, Tbilisi State University, Tbilisi; Georgia
- ¹⁵⁹ Department of Physics, Technion, Israel Institute of Technology, Haifa; Israel
- ¹⁶⁰ Raymond and Beverly Sackler School of Physics and Astronomy, Tel Aviv University, Tel Aviv; Israel
- ¹⁶¹ Department of Physics, Aristotle University of Thessaloniki, Thessaloniki; Greece
- ¹⁶² International Center for Elementary Particle Physics and Department of Physics, University of Tokyo, Tokyo; Japan
- ¹⁶³ Graduate School of Science and Technology, Tokyo Metropolitan University, Tokyo; Japan
- ¹⁶⁴ Department of Physics, Tokyo Institute of Technology, Tokyo; Japan
- ¹⁶⁵ Tomsk State University, Tomsk; Russia
- ¹⁶⁶ Department of Physics, University of Toronto, Toronto ON; Canada
- ¹⁶⁷ ^(a) TRIUMF, Vancouver BC; ^(b) Department of Physics and Astronomy, York University, Toronto ON; Canada
- ¹⁶⁸ Division of Physics and Tomonaga Center for the History of the Universe, Faculty of Pure and Applied Sciences, University of Tsukuba, Tsukuba; Japan
- ¹⁶⁹ Department of Physics and Astronomy, Tufts University, Medford MA; United States of America
- ¹⁷⁰ Department of Physics and Astronomy, University of California Irvine, Irvine CA; United States of America
- ¹⁷¹ Department of Physics and Astronomy, University of Uppsala, Uppsala; Sweden
- ¹⁷² Department of Physics, University of Illinois, Urbana IL; United States of America
- ¹⁷³ Instituto de Física Corpuscular (IFIC), Centro Mixto Universidad de Valencia – CSIC, Valencia; Spain
- ¹⁷⁴ Department of Physics, University of British Columbia, Vancouver BC; Canada
- ¹⁷⁵ Department of Physics and Astronomy, University of Victoria, Victoria BC; Canada
- ¹⁷⁶ Fakultät für Physik und Astronomie, Julius-Maximilians-Universität Würzburg, Würzburg; Germany
- ¹⁷⁷ Department of Physics, University of Warwick, Coventry; United Kingdom
- ¹⁷⁸ Waseda University, Tokyo; Japan
- ¹⁷⁹ Department of Particle Physics, Weizmann Institute of Science, Rehovot; Israel
- ¹⁸⁰ Department of Physics, University of Wisconsin, Madison WI; United States of America
- ¹⁸¹ Fakultät für Mathematik und Naturwissenschaften, Fachgruppe Physik, Bergische Universität Wuppertal, Wuppertal; Germany
- ¹⁸² Department of Physics, Yale University, New Haven CT; United States of America

^a Also at Borough of Manhattan Community College, City University of New York, New York NY; United States of America.

^b Also at Centro Studi e Ricerche Enrico Fermi; Italy.

^c Also at CERN, Geneva; Switzerland.

^d Also at CPPM, Aix-Marseille Université, CNRS/IN2P3, Marseille; France.

^e Also at Département de Physique Nucléaire et Corpusculaire, Université de Genève, Genève; Switzerland.

^f Also at Departament de Física de la Universitat Autònoma de Barcelona, Barcelona; Spain.

^g Also at Department of Financial and Management Engineering, University of the Aegean, Chios; Greece.

^h Also at Department of Physics and Astronomy, Michigan State University, East Lansing MI; United States of America.

ⁱ Also at Department of Physics and Astronomy, University of Louisville, Louisville, KY; United States of America.

^j Also at Department of Physics, Ben Gurion University of the Negev, Beer Sheva; Israel.

^k Also at Department of Physics, California State University, East Bay; United States of America.

^l Also at Department of Physics, California State University, Fresno; United States of America.

^m Also at Department of Physics, California State University, Sacramento; United States of America.

ⁿ Also at Department of Physics, King's College London, London; United Kingdom.

- ^o Also at Department of Physics, St. Petersburg State Polytechnical University, St. Petersburg; Russia.
- ^p Also at Department of Physics, University of Fribourg, Fribourg; Switzerland.
- ^q Also at Dipartimento di Matematica, Informatica e Fisica, Università di Udine, Udine; Italy.
- ^r Also at Faculty of Physics, M.V. Lomonosov Moscow State University, Moscow; Russia.
- ^s Also at Giresun University, Faculty of Engineering, Giresun; Turkey.
- ^t Also at Graduate School of Science, Osaka University, Osaka; Japan.
- ^u Also at Hellenic Open University, Patras; Greece.
- ^v Also at IJCLab, Université Paris-Saclay, CNRS/IN2P3, 91405, Orsay; France.
- ^w Also at Institució Catalana de Recerca i Estudis Avançats, ICREA, Barcelona; Spain.
- ^x Also at Institut für Experimentalphysik, Universität Hamburg, Hamburg; Germany.
- ^y Also at Institute for Mathematics, Astrophysics and Particle Physics, Radboud University Nijmegen/Nikhef, Nijmegen; Netherlands.
- ^z Also at Institute for Nuclear Research and Nuclear Energy (INRNE) of the Bulgarian Academy of Sciences, Sofia; Bulgaria.
- ^{aa} Also at Institute for Particle and Nuclear Physics, Wigner Research Centre for Physics, Budapest; Hungary.
- ^{ab} Also at Institute of Particle Physics (IPP), Vancouver; Canada.
- ^{ac} Also at Institute of Physics, Azerbaijan Academy of Sciences, Baku; Azerbaijan.
- ^{ad} Also at Instituto de Física Teórica, IFT-UAM/CSIC, Madrid; Spain.
- ^{ae} Also at Joint Institute for Nuclear Research, Dubna; Russia.
- ^{af} Also at Louisiana Tech University, Ruston LA; United States of America.
- ^{ag} Also at Moscow Institute of Physics and Technology State University, Dolgoprudny; Russia.
- ^{ah} Also at National Research Nuclear University MEPhI, Moscow; Russia.
- ^{ai} Also at Physics Department, An-Najah National University, Nablus; Palestine.
- ^{aj} Also at Physikalisches Institut, Albert-Ludwigs-Universität Freiburg, Freiburg; Germany.
- ^{ak} Also at The City College of New York, New York NY; United States of America.
- ^{al} Also at TRIUMF, Vancouver BC; Canada.
- ^{am} Also at Università di Napoli Parthenope, Napoli; Italy.
- ^{an} Also at University of Chinese Academy of Sciences (UCAS), Beijing; China.
- * Deceased.